This material has been copied
under licence from CANCOPY.
Resale or further copying of this material is
strictly prohibited.

Le présent document a été reproduit
avec l'autorisation de CANCOPY.
La revente ou la reproduction ultérieure
en sont strictement interdites.

HEAVY WATER EXPONENTIAL EXPERIMENTS USING ThO_2 and UO_2

by

J. A. THIE, Ph.D.

Argonne National Laboratory
Lemont, Illinois

PERGAMON PRESS
NEW YORK · OXFORD · LONDON · PARIS
1961

CONTENTS

I. INTRODUCTION 1
- Interest in oxide lattices 1
- Lattices investigated 2
- Types of lattice experiments 4
- Scope 4

II. THE EXPONENTIAL METHOD 8
- Types 8
- Single-zone theory 8
- Two group multizone theory 14
- Multizone perturbation theory 16
- Experimental techniques 17
- Example of buckling determination 19
- Corrections 21
- Precision of results 23

III. SCANDINAVIAN UO_2–D_2O LATTICE EXPERIMENTS 26
- Facility 26
- Lattice geometry 28
- Temperature coefficient 41
- Void coefficient 43
- Control rods 44
- Discussion 46

IV. INTERPRETATION OF SCANDINAVIAN UO_2–D_2O LATTICE EXPERIMENTS 48
- Introduction 48
- Fast effect 50
- Resonance escape probability 51
- Thermal utilization 52
- Migration areas 52
- Analysis of experiments 53
- Maximum of buckling curves 55
- Temperature coefficient 56

CONTENTS

V. SACLAY UO_2–D_2O LATTICE EXPERIMENTS 59
Facility 59
Substitution method 61
Lattice geometry 62
Bucklings 67
Discussion 71

VI. INTERPRETATION OF SACLAY UO_2–D_2O LATTICE EXPERIMENTS 75
Introduction 75
Fast effect 76
Resonance escape 81
Thermal utilization 83
Migration areas 84
The Saclay analysis of bucklings 86
The Chalk River analysis of bucklings 89

VII. SAVANNAH UO_2–D_2O LATTICE EXPERIMENTS 91
Facility 91
Lattice geometry 91
Bucklings 99
Discussion 106

VIII. INTERPRETATION OF SAVANNAH UO_2–D_2O LATTICE EXPERIMENTS 108
Introduction 108
Fast effect 111
Resonance escape 112
Thermal utilization and η 113
Migration area 114
Analysis of bucklings 117

IX. ARGONNE UO_2–ThO_2–D_2O LATTICES 119
Facility 119
Lattice geometry 122
Bucklings 124
Buckling coefficients 127

X. THEORETICAL INTERPRETATION OF UO_2–ThO_2–D_2O LATTICES 129
Multigroup theory 129
Fast effect 133

Resonance capture 133
Epithermal capture 135
Thermal capture 137
Age 137
Thermal migration area 139
Bucklings 140

XI. Considerations in Planning Exponentials 144
Need for experiment 144
Type of experiment 146
Fuel element 148
Lattice 149
Tank 150
Source 152
Flux distribution methods 152
Safety 153
Data processing 155

Appendix A 156

Appendix B 160

Appendix C 163

Appendix D 167

Index 169

CHAPTER III

SCANDINAVIAN UO_2–D_2O LATTICE EXPERIMENTS

Facility

Exponentials for heavy water lattice fueled with natural uranium in the form of UO_2 have been conducted during 1957 and 1958 at the AB Atomenergi Laboratory in Stockholm, Sweden.[1, 2] This was a joint effort of the Swedish AB Atomenergi and the Dutch–Norwegian Joint Establishment for Nuclear Energy Research (JENER). Both experimental personnel and lattice materials were contributed by both organizations. One of the incentives in this Scandinavian effort was obtaining data for clustered lattice likely to be used in the Norwegian Halden boiling reactor.[3]

Figure 3-1 shows the ZEBRA (Zero Energy Base Reactor Assembly) exponential at the AB Atomenergi Laboratory. It can be seen that the lattice and source were in a lower room, while the electronics and loading mechanisms were in a room above. The 15 ft dimensions of the lower room gave rise to fast neutron reflections, and location near reactor, *R*1, sometimes caused large background effects. However, these effects were coped with by carefully made corrections, and the taking of data when *R*1 was not in operation.

The aluminum tank in Fig. 3-1 was 3 m high and 0·999 m inside diameter. Its 1 cm wall was covered with 0·4 cm of polyethylene containing 0·3 gms of boron carbide per cm^2. This helped to provide a black boundary for fast as well as thermal neutrons. The effective radius for *thermal neutrons* is the sum of the tank inner radius, $R_0 = 49{\cdot}95$ cm, and λ_r. The latter is the sum of the extrapolation length of D_2O, 1·77 cm, and the boundary's reflector savings, 0·37 cm, or 2·14 cm. Hence,

$$R = 49{\cdot}95 + 2{\cdot}14 = 52{\cdot}09 \text{ cm.} \qquad (3\text{-}1)$$

The effective radius of *epithermal neutrons* is somewhat larger because the transport cross-section is smaller. The value of the radius wanted is, however, for *pile neutrons*, i.e. a mixture of thermal and epithermal neutrons, and therefore depends on the lattice arrangement (or the cadmium ratio). The effective radius of pile

neutrons in different lattices has been calculated by means of two-group theory.[4]

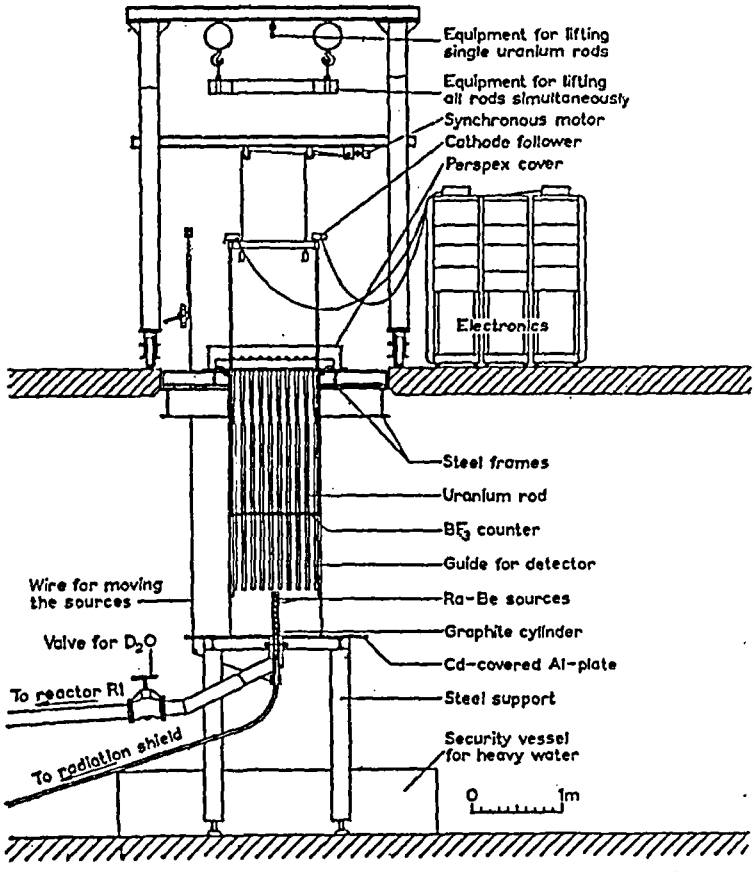

FIG. 3-1. Experimental arrangement of the Scandinavian exponential.

To allow temperature coefficient measurements the system was equipped with a 30 kW electric heater, a tap water heat exchanger as a cooler, and a circulating pump. A temperature range of 10 °C to 80 °C could be studied.

A fuel rod was suspended from an aluminum wire wrapped around a roller which rests in grooves in a horizontal beam at the top of the tank. As shown in Fig. 3-2 these beams are chords of a circle and

are continuously variable in location. This arrangement allowed a high degree of lattice flexibility, yet rapid lattice changes.

The source used was a 1 curie Ra–Be. Its point location at the bottom of the fuel rods led to flux harmonics in the lower part of the assembly. However, by using a 35 cm long, 1 cm diameter BF_3 proportional counter, it was possible to eliminate the harmonics by

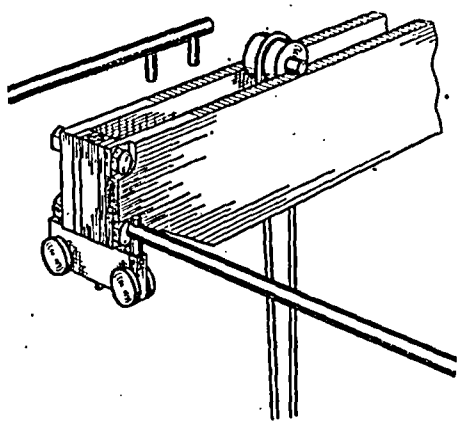

FIG. 3-2. Details of the suspension of the fuel rods.

integration. This was done during axial flux distributions locating the counter along a diameter between r_1 and r_2 such that inner nodes of the second and third harmonics fall within r_1 and r_2.

For axial flux distributions the bottom arm of a U-shaped pipe shown in Fig. 3-1 contained two counters symmetrically located on a diameter. Wires leading to a synchronous motor allowed a 1 cm/min vertical motion of the probe. Count recordings at 5 to 15 min intervals were automatically made, and statistical accuracy of 0·1 per cent was readily attainable.

Lattice geometry

The seventy-one lattices investigated by Persson *et al.* used clusters of 6, 7, 13 and 19 rods 1·56 cm in diameter, and also clusters of 6, 7, 19 and 27 rods 1·22 cm in diameter. Cross-sectional views of these fuel elements are shown in Figs. 3-3 to 3-7. Efforts were made to keep the air volumes between UO_2 and the clad to a minimum.

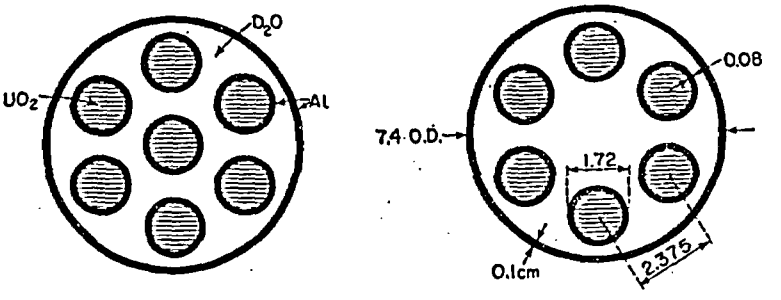

FIG. 3-3. Six and seven rod clusters used in lattices 1 through 20 of the Scandinavian exponential (all dimensions are in cm).

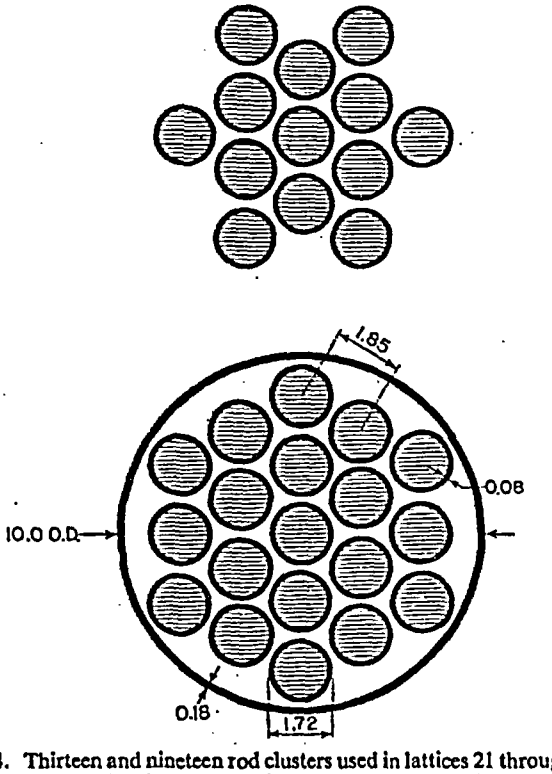

FIG. 3-4. Thirteen and nineteen rod clusters used in lattices 21 through 28 of the Scandinavian exponential (all dimensions are in cm).

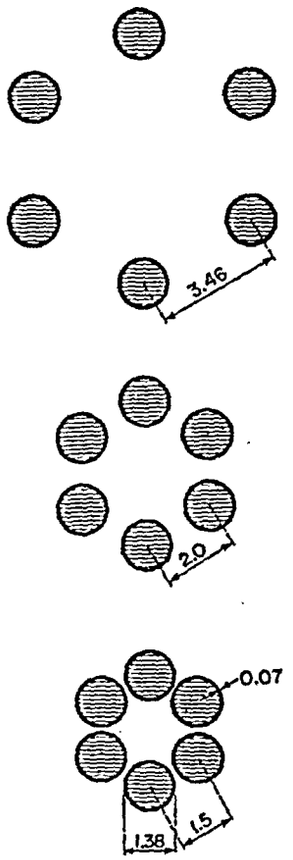

FIG. 3-5. Six rod clusters used in lattices 29 through 36d of the Scandinavian exponential (all dimensions are in cm).

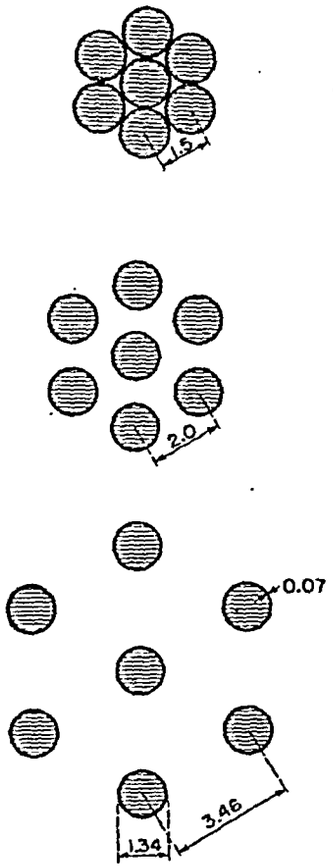

FIG. 3-6. Seven rod clusters used in lattices 37 through 48 of the Scandinavian exponential (all dimensions are in cm).

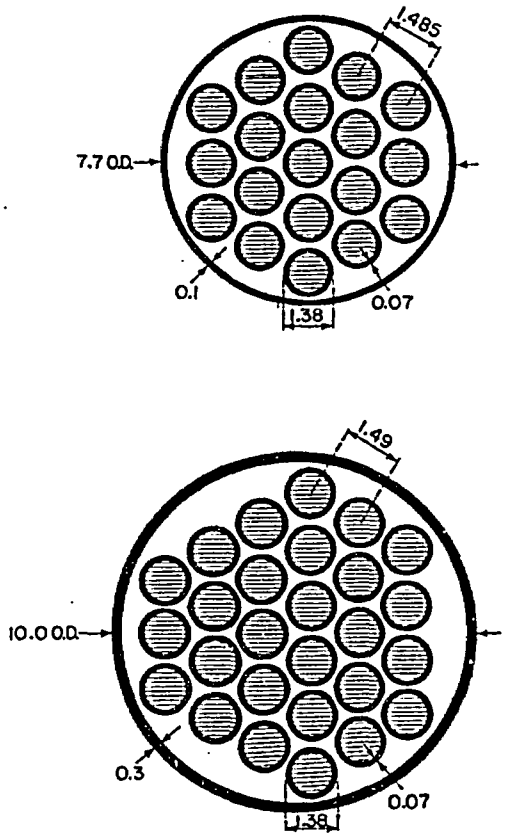

FIG. 3-7. Nineteen and twenty-seven rod clusters used in lattices 48a through 53 of the Scandinavian exponential (all dimensions are in cm).

Lattices constructed from these fuel elements had hexagonal spacings ranging from 12 to 30 cm between fuel element centers. A complete summary of the dimensional specifications of these lattices is found in Table 3-1. Note that the grams of natural uranium oxide per unit height is specified instead of a density to avoid ambiguity. Three conventions exist for the unit of fuel volume in giving fuel densities:

(a) a volume based on average micrometer measurements of pellets;

TABLE 3-1. DIMENSIONS OF THE SCANDINAVIAN LATTICES

Lattice No.	O.D. of UO_2 in cm	I.D. of clad in cm	Thickness of clad in cm	Grams of UO_2 per cm	Number of rods	Spacing of rods in cm	I.D. of shroud in cm	Thickness of shroud in cm	Spacing of fuel element in cm
1									12
2									14
3									16
4									18
5					6	2·375	7·2	0·1	20
6									22
7									24
8									26
9									28
10									30
11									12
12									14
13									16
14	1·56	1·56	0·08	18·0	7	2·375	7·2	0·1	18
15									20
16									22
17									24
18									26
19									28
20									30
21									16
22					13	1·85	—	—	20
23									24
24									20
25									22
26					19	1·85	9·64	0·18	24
27									26
28									28
29									12
30					6	1·5	—	—	14
31									16
32									18
33									12
34					6	2·0	—	—	14
35									16
36									18
36a									12
36b					6	3·46	—	—	14
36c									16
36d									18
37									12
38					7	1·5	—	—	14
39									16
40									18
41	1·22	1·24	0·07	11·2					12
42					7	2·0	—	—	14
43									16
44									18
45									12
46					7	3·46	—	—	14
47									16
48									18
48a									18
48b									20
48c									22
48d									24
48e									26
48f									28
48g					19	1·485	7·5	0·1	30
48h									18
48i									20
48j									22
48k									24
48l									26
48m									28
48n									30
49									20
50									22
51					27	1·49	9·4	0·3	24
52									26
53									28

(b) a volume determined from an average weight loss by weighing pellets in air and in a liquid;
(c) a volume based on average measurements of the inner boundary of the cladding.

According to the third convention the 18 and 11·2 g of UO_2 per cm of height in Table 1 correspond to densities of 9·42 and 9·27 g/cm^3 respectively.

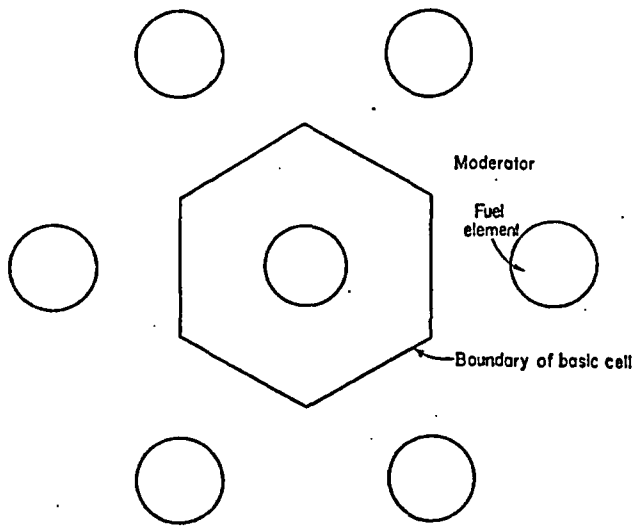

FIG. 3-8. Cross-sectional view of the basic lattice cell.

Table 3-2 gives the volume fractions and ratios of these lattices. The basic lattice cell of Fig. 3-8 is a hexagon of area 0·866 times the square of the full element spacing. Such a cell has one complete fuel element cluster at its center.

Table 3-2 also gives the material bucklings. In these measurements $(2{\cdot}4048/R)^2$ was in the vicinity of 2100μB. Although the statistical error of the bucklings is less than 10μB, the total error, including possible systematic errors is believed to be less than 20μB.

The exponentials were all of the single zone type except lattices 1, 11 and 12. There were two-zone exponentials in which the radius of the central zone was varied. The outer zone used 3·05 cm diameter natural uranium metal rods in its lattice. In addition lattices 2

TABLE 3-2. VOLUMES AND BUCKLINGS OF THE SCANDINAVIAN LATTICES

Lattice No.	Volume in cm³ in a lattice cell 1 cm high					D_2O volume ÷ fuel space*	Al volume ÷ fuel space*	B^2 in μB
	Fuel space*	Clad	Shroud	D_2O				
				Internal	External			
1					81·7	9·46		316
2					126·7	13·39		479
3					178·7	17·92		527
4					237·6	23·05		513
5	11·47	2·473	2·293	26·77	303·4	28·79	0·416	473
6					376·1	35·13		425
7					455·8	42·08		376
8					542·4	49·63		326
9					635·9	57·79		284
10					736·4	66·55		239
11					81·7	7·93		236
12					126·7	11·30		447
13					178·7	15·18		519
14					237·6	19·58		525
15	13·38	2·885	2·293	24·45	303·4	24·50	0·387	496
16					376·1	29·94		443
17					455·8	35·90		400
18					542·4	42·37		354
19					635·9	49·36		301
20					736·9	56·87		258
21				191·5		7·71		361
22	24·85	5·358	0	316·2		12·73	0·216	577
23				468·6		18·86		562
24					267·9	8·17		395
25					340·6	10·17		460
26	36·32	7·831	5·553	28·84	420·3	12·37	0·369	488
27					506·9	14·75		490
28					600·4	17·33		464
29				115·7		15·97		584
30				160·7		22·19		582
31				212·7		29·36		531
32	7·246	1·729		271·6		37·49		461
33				115·7		15·97		556
34				160·7		22·19		574
35				212·7		29·36		527
36				271·6		37·49		463
36a				115·7		15·97		548
36b				160·7		22·19		577
36c				212·7		29·36		541
36d				271·6		37·49		482
37				114·2		13·51		573
38			0	159·2		18·84	0·2386	596
39				211·2		24·99		562
40				270·1		31·95		495
41				114·2		13·51		528
42	8·453	2·017		159·2		18·84		580
43				211·2		24·99		555
44				270·1		31·95		495
45				114·2		13·51		482
46				159·2		18·84		558
47				211·2		24·99		531
48				270·1		31·95		493
48a					234·0	10·20		535
48b					299·8	13·07		554
48c					372·6	16·24		561
48d				0	452·3	19·71		540
48e					538·9	23·49		497
48f					632·4	27·56		446
48g	22·95	5·474	2·388		732·9	31·94	0·3426	410
48h					234·0	10·89		494
48i					299·8	13·76		531
48j					372·6	16·93		526
48k				15·76	452·3	20·40		501
48l					538·9	24·17		465
48m					632·4	28·25		409
48n					732·9	32·63		366
49					267·9	9·11		352
50					340·6	11·33		405
51	32·61	7·779	9·142	29·02	420·3	13·77	0·519	429
52					506·9	16·43		424
53					600·4	19·30		398

* The fuel space is a volume 1 cm high and bounded by the inner boundary of the clad.

and 13 were measured by both the two-zone and single-zone methods in order to verify the method of analysis for the former.

Figures 3-9 to 3-15 show the bucklings of these lattices as a function of the D_2O to UO_2 volume ratio. The volume used for the latter is the space defined by the inner surface of the clad (not the

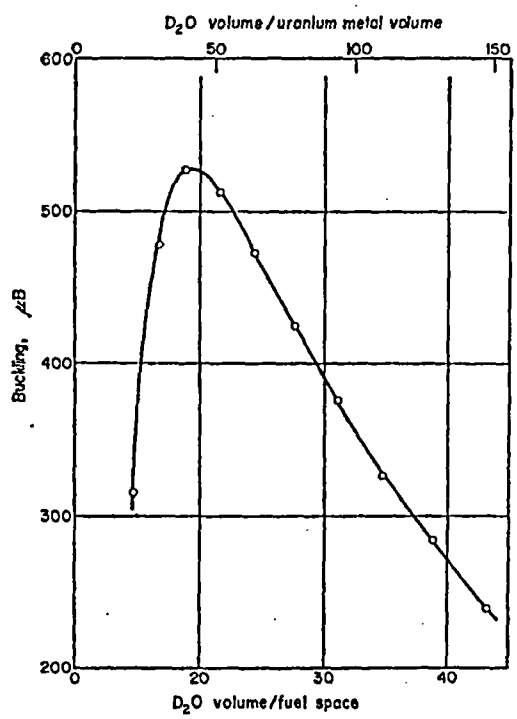

FIG. 3-9. Bucklings of clusters of six 1·56 cm diameter UO_2 rods (shown in Fig. 3-3).

outside diameter of the fuel). Since various experiments use oxides of various densities and air gaps of various sizes, the abscissae also show the D_2O volume per unit volume of equivalent metal. This is the volume ratio that would exist in a 18·7 g/cm^3 uranium metal – D_2O lattice having the same atomic ratio of uranium and deuterium as the lattice measured. This type of data presentation is conventional, and also convenient for showing effects of heterogeneity.

The maximum exhibited in these curves is quite typical of buckling measurements in heterogeneous reactors. That an optimum might

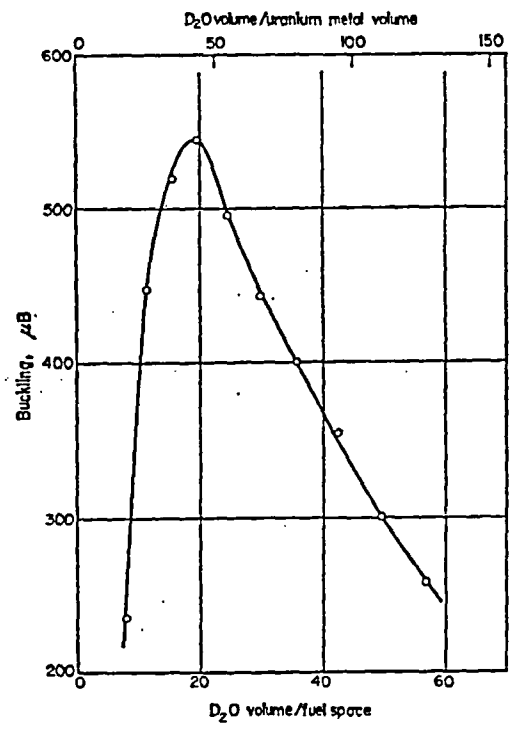

FIG. 3-10. Bucklings of clusters of seven 1·56 cm diameter UO_2 rods (shown in Fig. 3-3).

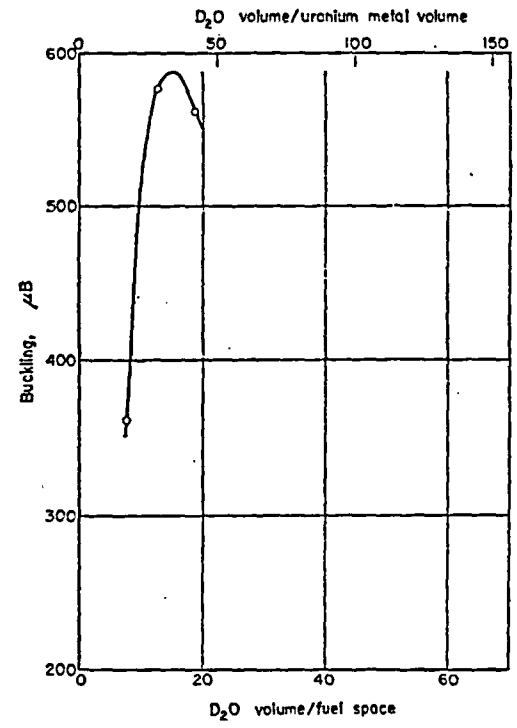

FIG. 3-11. Bucklings of clusters of thirteen 1·56 cm diameter UO_2 rods (shown in Fig. 3-4).

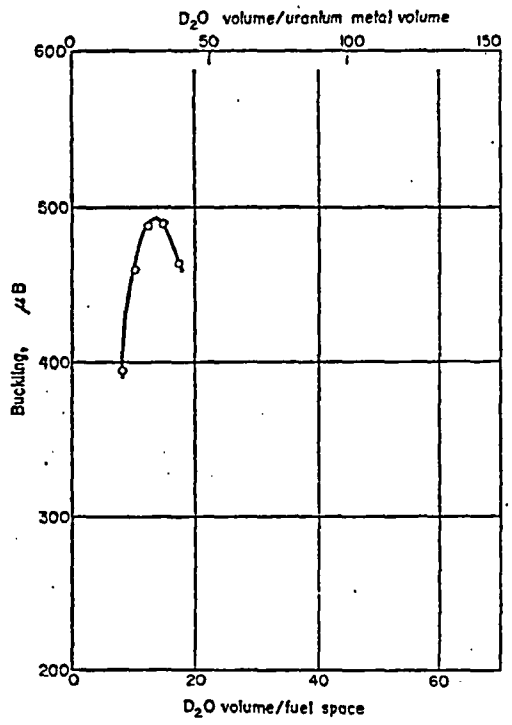

FIG. 3-12. Bucklings of clusters of nineteen 1·56 cm diameter UO_2 rods (shown in Fig. 3-4).

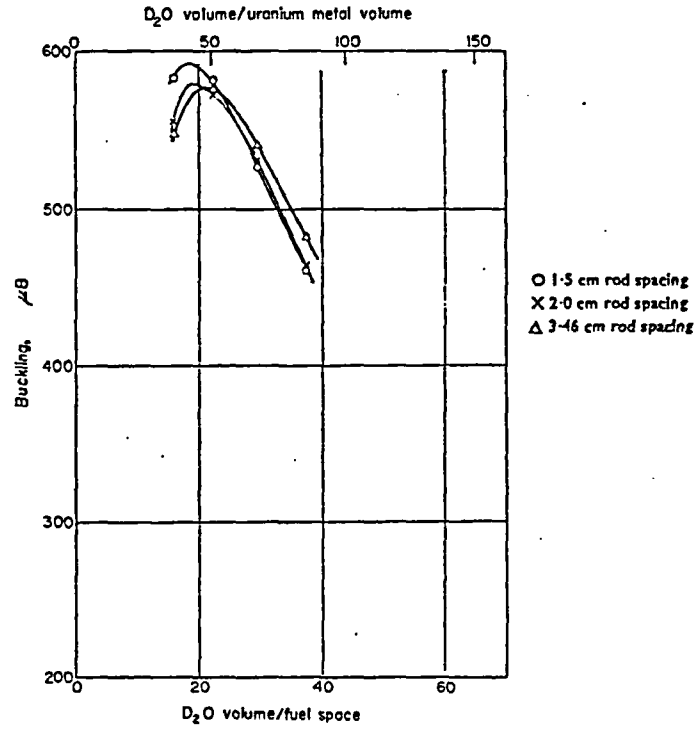

FIG. 3-13. Bucklings of clusters of six 1·22 cm diameter UO_2 rods (shown in Fig. 3-5).

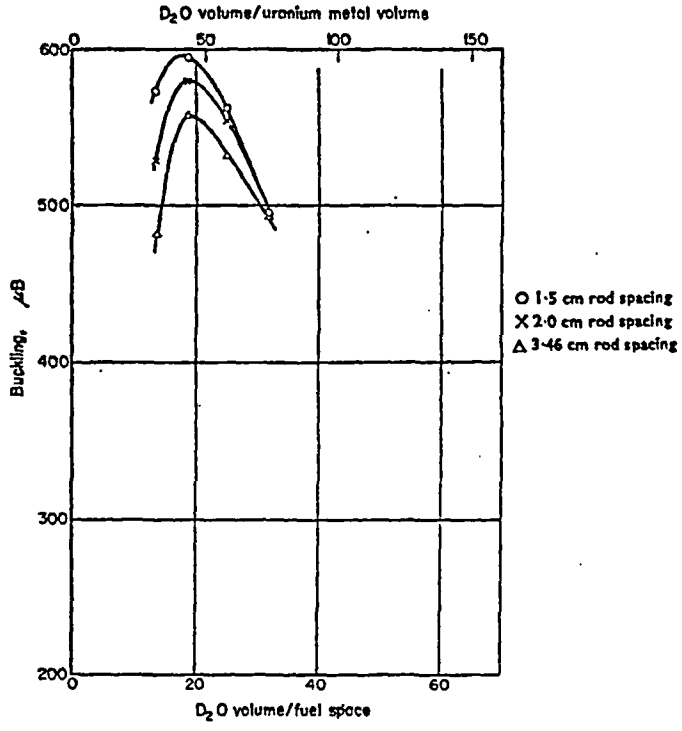

FIG. 3-14. Bucklings of clusters of seven 1·22 cm diameter UO_2 rods (shown in Fig. 3-6).

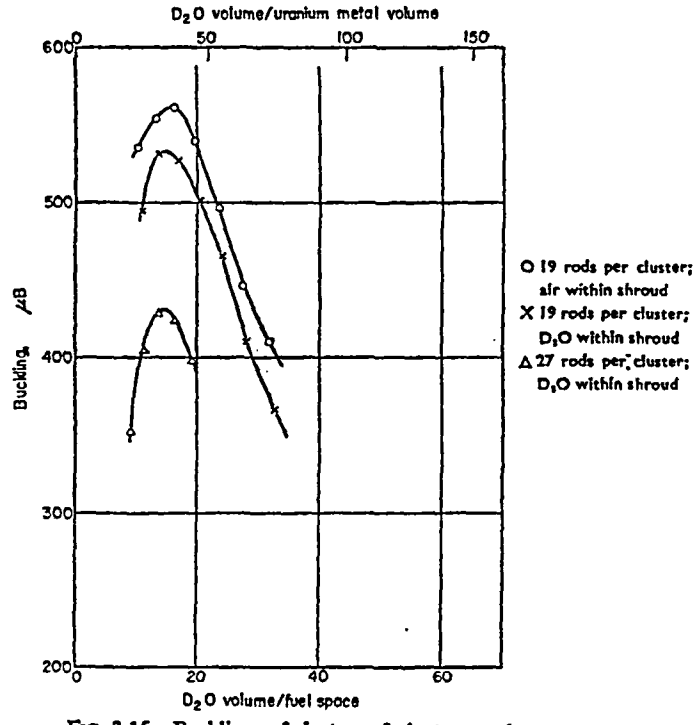

FIG. 3-15. Bucklings of clusters of nineteen and twenty-seven 1·22 cm diameter UO_2 rods (shown in Fig. 3-7).

exist is reasonable from purely physical consideration. At very low moderator to fuel ratios, resonance capture is very high due to lack of moderation; at very high moderator to fuel ratios, thermal migration distances and thermal captures are large in the excessive moderator volume. Both effects lead to low bucklings. It can be expected that a buckling maximum is attained at intermediate moderator to fuel ratios. Chapter IV and Appendix C discuss this more quantitatively.

In some cases, as for example Fig. 3-11, the data defining the traditional buckling curve is somewhat sparse. It is nevertheless possible to pass a curve through the data which is more than just a guess. Theoretical considerations in Appendix C indicate that in the vicinity of buckling maxima, the nature of the curve is approximately of the form:

$$B^2 = -A_1 x + A_2 - \frac{A_3}{x} \tag{3-2}$$

where x is the moderator to fuel ratio. Therefore a curve based on Equation (3-2) is used to connect the measured bucklings in this as well as succeeding chapters. When more than three bucklings are measured, a reasonable method is to base the connecting curve on Lagrangian interpolation of the function xB^2, as discussed in Appendix C.

Figures 3-16 and 3-17 show buckling differences obtained from this data. In the former it is seen that whether there is a buckling gain or loss by adding a fuel rod to a cluster is dependent on whether the lattice is overmoderated or undermoderated respectively. Also the condition for no effect, $\Delta B^2 = 0$, at a moderator to fuel space ratio of about 20, agrees with the location of the maxima of previous 6 and 7 rod buckling curves. The reason for the higher buckling of the tighter spacing at low moderator to fuel ratio in Fig. 3-17 essentially stems from decreased resonance capture. This is discussed further in Chapter IV.

During the course of the experiments, measurements of the purity of the heavy water were made. It was found that its purity decreased from 99·75 to 99·65 per cent in two years. Measurements of L^2 of this heavy water also decreased from 9600 ± 1200 to 8100 ± 1100. The buckling values here probably more nearly correspond to heavy water of the lower purity.

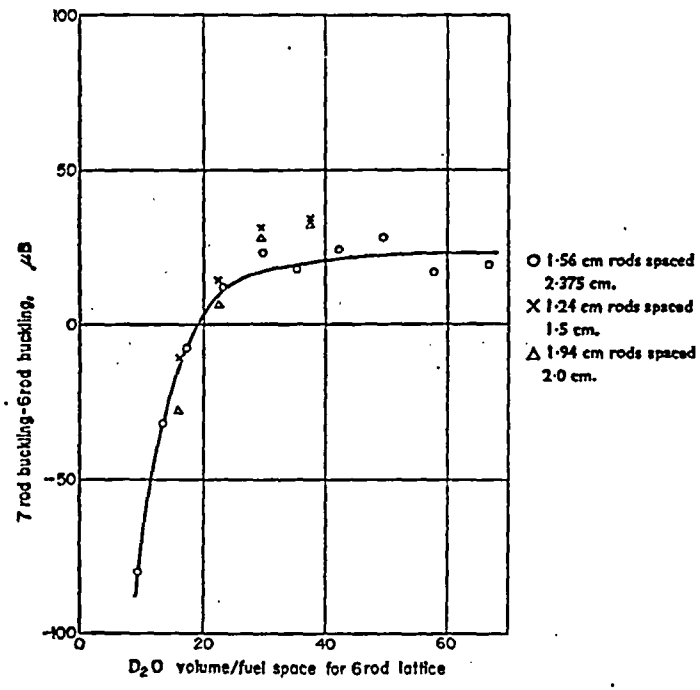

FIG. 3-16. Change in buckling by adding a central rod to a six rod cluster.

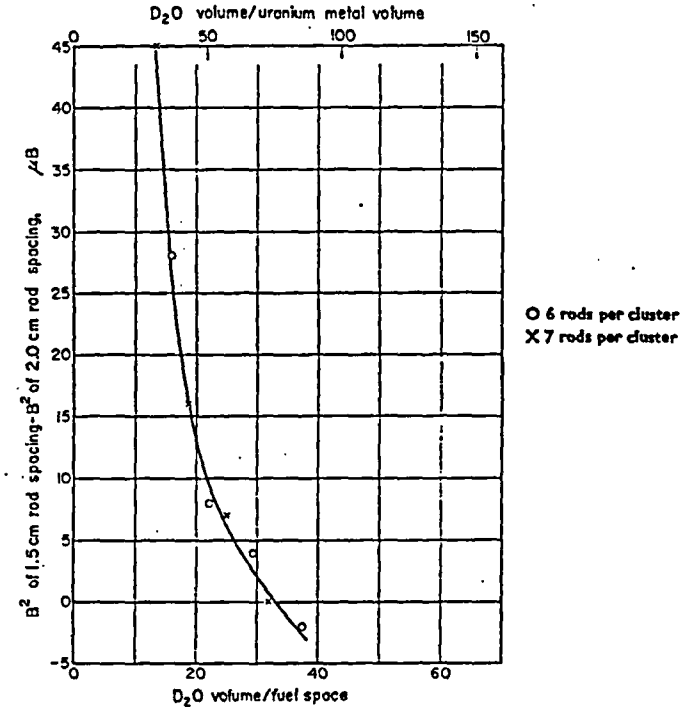

FIG. 3-17. Buckling difference between lattices of 1·5 cm and 2·0 cm rod spacings.

Temperature coefficient

Experimentally it was possible to determine differences in κ, the axial flux attenuation constant, quite accurately. Therefore a temperature coefficient of buckling measurement was based on this principle. A differentiation of the basic expression for buckling, Equation (2-14) gives

$$\frac{dB^2}{dT} = \frac{dB_r^2}{dT} - 2\kappa\frac{d\kappa}{dT}. \tag{3-3}$$

For the Scandinavian exponential, the first term contributes only about 20 per cent to the total temperature coefficient. Therefore, it can be treated as a correction and computed from theory.[1]

If the background corrected axial flux distributions, $\phi_1(z)$ and $\phi_2(z)$ are measured at two temperatures, T_1 and T_2, then from Equation (2-4):

$$\phi_1(z) = A_1 \sinh \kappa_1(H-z) \tag{3-4}$$

$$\phi_2(z) = A_2 \sinh \kappa_2(H-z) \tag{3-5}$$

$$\left.\begin{aligned} \ln\frac{\phi_1(z)}{\phi_2(z)} &= \ln\frac{A_1}{A_2} + \ln\frac{\sinh \kappa_1(H-z)}{\sinh \kappa_2(H-z)} \\ &= \ln\frac{A_1}{A_2} + (\kappa_1-\kappa_2)H + (\kappa_2-\kappa_1)z + \\ &\qquad + \ln\frac{1-\exp[-2\kappa_1(H-z)]}{1-\exp[-2\kappa_2(H-z)]}. \end{aligned}\right\} \tag{3-6}$$

In most exponentials, measurements are made in regions where $\kappa(H-z)$ is somewhat greater than 1. Thus, the last term is small and $\kappa_2 - \kappa_1$ can be readily had from the linear dependence of $\ln[\phi_1(z)/\phi_2(z)]$ on z. The desired $d\kappa/dT$ is:

$$\frac{d\kappa}{dT} = \frac{\kappa_2-\kappa_1}{T_2-T_1} \tag{3-7}$$

Figure 3-18 shows the results of determining $d\kappa/dT$ from Equations (3-6) and (3-7), then dB^2/dT from (3-3). The lattice chosen was the 19 rod and cluster of Fig. 3-4 in a 22 cm square lattice. This is virtually equivalent to a hexagonal spacing of 23·64 cm, both in volume ratios and bucklings. The buckling of 487μB from Table 3-3 compares well with the 484μB from Fig. 3-12 for the hexagonal equivalent.

Figure 3-18 also shows the temperature coefficient of L^2 of D_2O. If a buckling measurement is made in an assembly having no fissionable material then

$$B^2 = -\frac{1}{L^2}. \tag{3-8}$$

This is because $k_\infty = 0$ and $\tau = 0$ in Equation (2-5).

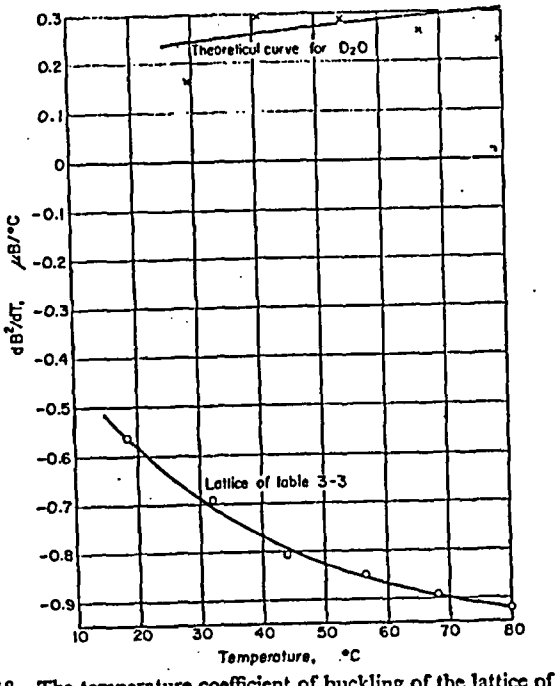

FIG. 3-18. The temperature coefficient of buckling of the lattice of Table 3-3, and the temperature coefficient of L^2 of D_2O.

In regard to the precision obtained, it is believed that $d\kappa/dT$ was measured to within 3 per cent in the middle of the temperature range covered. However, dB^2/dT is not known quite this accurately because of errors in dB_r^2/dT correction and perhaps other systematic errors. Also the temperature coefficient of L^2 of D_2O is somewhat less accurate than this.

Void coefficient

Lattices 48a through 48n shown in Fig. 3-15 are seen to display the effect of the coolant D_2O within the shroud. (These lattices, along with 36a through 36d, are presented here prior to their publication, through the courtesy of R. Persson of AB Atomenergie.)

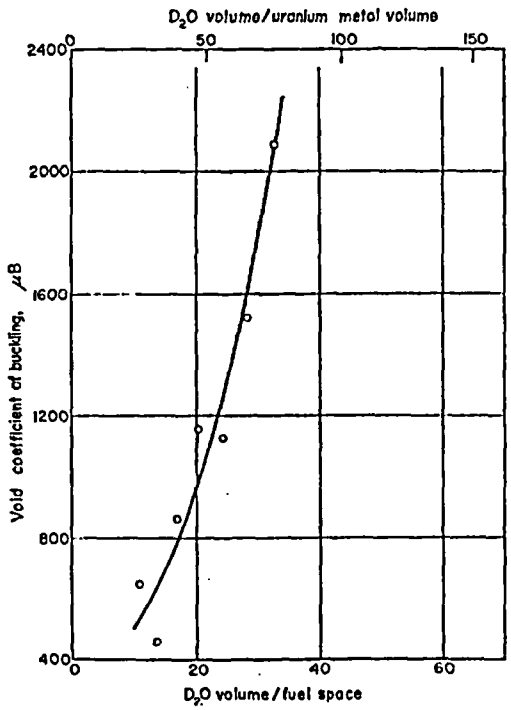

FIG. 3-19. Void coefficient of buckling for the nineteen rod cluster.

A quantity somewhat analogous to the temperature coefficient is the void coefficient of buckling. It can be defined as the increase in buckling divided by the fraction of the total heavy water present which is replaced by void or air.

Fig. 3-19 shows this coefficient as obtained by subtracting the measured bucklings with and without the internal D_2O. In spite of the small difference being measured, the scatter of points about the curve is not excessive. However, this experiment is a difficult

one to interpret. Small anisotropies due to voided channels, as seen below in Equation (3-9), can affect results substantially.

Voids can influence the buckling in either a positive or a negative way, depending on their location in the lattice, and the relative importance of the various thermal, resonance and fast neutron processes. Void coefficient experiments such as this can offer rather stringent tests to theoretical models being used for such things as the fast effect and the Dancoff correction for the resonance capturing surface. These are known from qualitative considerations to explain positive void coefficients, due to void near the fuel.

Control rods

Although the worth of control rods is generally measured in critical rather than exponential assemblies, measurements in the latter do have merit: comparisons can be made with *a priori* theories; and extrapolations to critical systems are possible.[1] A single rod along the entire central axis of the exponential assembly is the simplest and most meaningful experiment. The difference in axial bucklings with and without this control rod may be interpreted as a change in radial buckling for the particular tank used.

Figure 3-20 shows two control rods used. These were inserted between the fuel clusters of the lattice of Table 3-3, and also in a

TABLE 3-3. CHARACTERISTICS OF LATTICE USED FOR TEMPERATURE COEFFICIENT MEASUREMENTS

O.D. of UO_2	1·56 cm
I.D. of clad	1·56 cm
Thickness of clad	0·08 cm
No. of rods within shroud	19
Hexagonal spacing of rods	1·85 cm
I.D. of shroud	9·64 cm
Thickness of shroud	0·18 cm
Square spacing of clusters	22 cm
Buckling at 18·4°C	487μB

tank of D_2O. It should be noted that there is heavy water internal to the cadmium. Therefore not only is the cadmium black to thermal neutrons, but fast neutrons thermalized in the interior are also captured.

The inferred increase in radial buckling in the 99·9 cm I.D. tank due to the insertion of these control rods is given in Table 3-4.

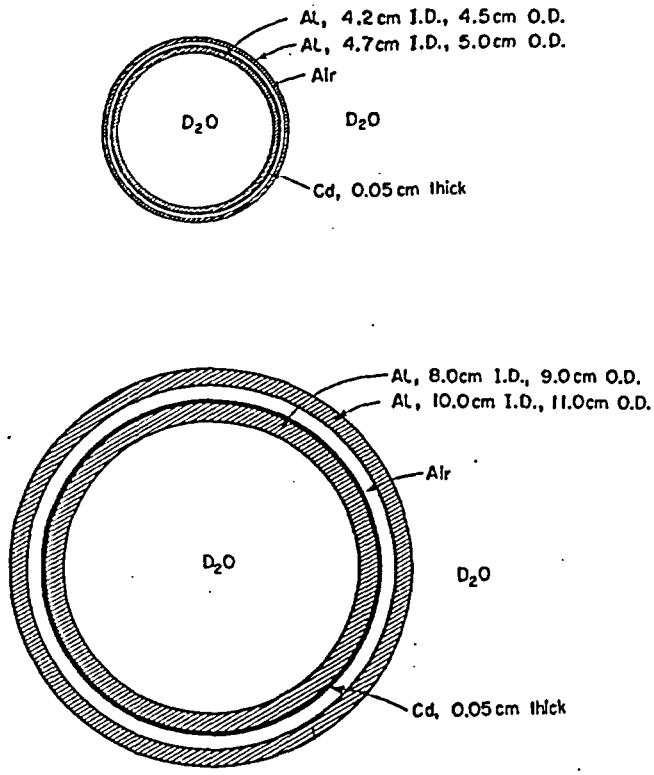

FIG. 3-20. Cross-sectional views of control rods inserted into the Scandinavian exponential.

TABLE 3-4. BUCKLING CHANGES DUE TO CONTROL ROD INSERTION

Lattice	Buckling of lattice in μB	O.D. of Cd in cm	ΔB_r^2 in μB
(See Table 3-3)	482	4·6	510 ± 20
		9·1	840 ± 30
D_2O	−105	4·6	780 ± 50
		9·1	1350 ± 60

Discussion

The experimental methods used in this set of exponential experiments on the whole proved quite satisfactory. In particular the motor-driven detection systems using automatically recorded BF_3 counters was felt to be quite successful. Good counting statistics

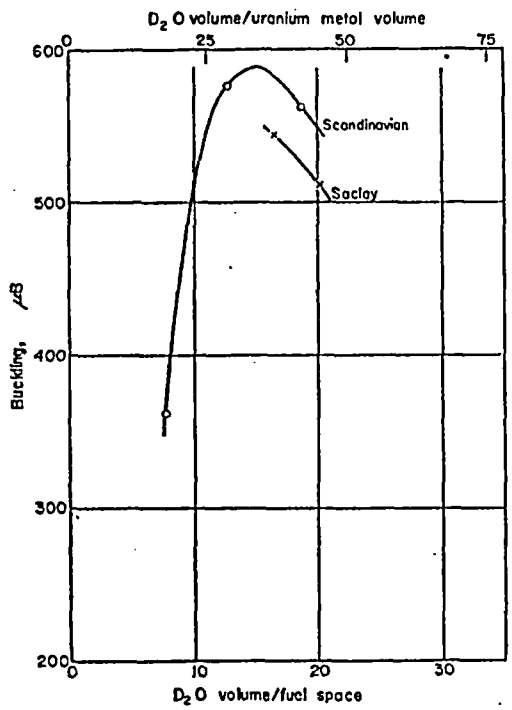

FIG. 3-21. Comparison of Scandinavian and Saclay buckling measurements of the same thirteen rod clusters (Fig. 3-4).

from a relatively weak source was possible: 0·1 per cent statistical accuracy from a 1 curie Ra–Be source.

During most of the measurements the precision was limited by hard gamma-rays and fast neutrons from an adjacent reactor, R1. This is one of the chief reasons the total error of the bucklings is estimated at $\pm 20\mu B$. Nevertheless, acceptable accuracy was attained on temperature coefficient and control rod worth measurements.

The French zero power reactor, Aquilon, at Saclay has made some measurements[5] with the same fuel elements used in Scandinavian exponential. Except for the fact that the Saclay lattices used square instead of hexagonal spacing of the clusters, the lattices were identical. It has already been noted that the square spacing (the lattice of Table 3-3) is experimentally equivalent to a hexagonal spacing having the same volume ratios. The comparison is made in Fig. 3-21. The Saclay bucklings are about 35μB smaller than the Scandinavian values. One explanation for this systematic discrepancy could be an uncertainty in radial buckling.

Persson[1] has noted that a small anisotropy in neutron diffusion could also account for the difference. If the migration area, $M^2 = \tau + L^2$, is different in the z direction than the r direction, then Equation (2-14) must be replaced by

$$M_r^2 B_r'^2 + M_z^2 B_z'^2 = M_r^2 B_r^2 - M_z^2 \kappa^2 \tag{3-9}$$

if an exponential characterized by B_r^2 and κ^2 is to be compared with the same lattice in another geometry characterized by $B_r'^2$ and $B_z'^2$. Since $B_r^2 - \kappa^2$ is about $\frac{1}{5}$ of B_r^2 for these Scandinavian lattices a 2 per cent difference between M_r^2 and M_z^2, (if such an amount exists), is magnified five-fold. This could also account for the discrepancy between these measurements and those of Saclay. In the latter $B_z'^2$ and $B_r'^2$ are of the same order.

REFERENCES

1. R. Persson *et al.*, Exponential experiments on heavy water–natural uranium metal and oxide lattices, P/160. Geneva conference (1958).
2. E. Andersen and O. Aspelund, Exponential experiments with uranium oxide clusters in heavy water, P/575. Geneva conference (1958).
3. N. Hidle and O. Dahl, The Halden boiling heavy water reactor, P/559. Geneva conference (1958).
4. R. Persson *et al.*, Exponential pile experiments with natural uranium and heavy water, *J. Nucl. Engng.*, 3, 188 (1956).
5. Y. Girand *et al.*, Natural uranium–heavy water lattices, P/336. Geneva conference (1958).

CHAPTER IV

INTERPRETATION OF SCANDINAVIAN $UO_2 - D_2O$ LATTICE EXPERIMENTS

Introduction

The experiments performed at Stockholm had as a goal the obtaining of information necessary for a basic understanding of uranium oxide fueled heavy water moderated reactors. A purpose of this nature is encountered in virtually all exponential and critical experimental programs. It is to be contrasted with the intent of the so-called " mock-up " experiments. The latter, useful in their own right, have as a primary purpose the obtaining of some specific number (such as critical size, enrichment, etc.) applicable only to the design of a specific reactor.

To obtain a basic understanding of the data of the previous chapter requires a comparison with reactor theory. The extent to which a given method is successful in arriving at buckling results given by experiment, is an indication of the mutual success of the theory and the experiment. However, another indication of the trustworthiness of a theoretical model which explains an experiment has to do with the range of the experiment and the degree to which the theory contains empiricisms. For example, it is highly satisfactory if a truly *a priori* theory gives bucklings in good agreement with those measured for many fuel elements having many spacings. At the other extreme, it is rather unsatisfactory if the only theoretical interpretation consists in determining n parameters empirically to obtain a fit to n bucklings.

Most exponential experiments are evaluated by an approach which is a compromise between a completely basic and a completely empirical approach. η, the number of neutrons per thermal capture in the fuel, and the resonance integral of the fertile material are typically chosen as parameters to be determined by fitting the theory to the experiment. Pershagen, Anderson, and Carlvik[1] in their analysis chose η as the parameter to be determined in the age-diffusion equations,

$$D_s \nabla^2 \phi_s - \sum_{as} \phi_s + q(\tau) = 0 \qquad (4\text{-}1)$$

$$\nabla^2 q = \frac{\partial q}{\partial \tau} \tag{4-2}$$

$$q(0) = \varepsilon \eta f p \sum_{as} \phi_s \tag{4-3}$$

Here $q(\tau)$ is the source of neutrons for the thermal group. The four-factor formula is adopted, in which k_∞ is the product of: the fast fission factor, ε; η; the thermal utilization, f; and the resonance escape, p.

If $\nabla^2 \phi_s$ is taken to be $-B^2\phi_s$ and $\nabla^2 q$ to be $-B^2 q$, then these equations lead in a straight forward fashion to the following solutions for the flux and its source:

$$\phi_s = \frac{q(\tau)}{\sum_{as}(1+L^2B^2)} \tag{4-4}$$

$$q(\tau) = k_\infty \sum_{as} \phi_s e^{-\tau B^2} \tag{4-5}$$

Elimination of ϕ_s and $q(\tau)$ leads to the age-diffusion critical equation,

$$k_\infty = \varepsilon \eta p f = e^{\tau B^2}(1+L^2B^2) \tag{4-6}$$

With the parameters, ε, p, f, τ and L^2, computed for each lattice whose buckling, B^2, has been measured, it is possible to solve for η by means of Equation (4-6).

The methods used in computing ε, p, f, τ and L^2 are given in some detail here. This is necessary for the resulting η determined to have meaning. It will be the η, which, if used with the other lattice constants computed by these methods, gives bucklings in more or less agreement with experiment. The extent to which agreement is possible depends on:

(a) the average deviation among the η's determined by the experiment;

(b) the degree to which the lattice being computed represents an extrapolation from the lattices measured.

It is also instructive to look at methods of computing lattice constants as given by various groups: the Swedish and JENER groups here, and other groups in succeeding chapters. Except possibly for methods such as monte carlo (which is merely a precise mathematical simulation of the experiment), it will be seen in this and the chapters to follow that the variation in reactor calculational techniques is significant. This stems largely from different groups desiring different degrees of balance between theoretical precision and simplicity of computation. To a lesser extent it is due to judgements concerning approximate methods differing.

One practical application of the Scandinavian exponential experiment is to allow accurate calculations to be made for the Halden boiling reactor.[2] Since the Halden fuel element type was among those studied, and since the temperature coefficient of buckling was also measured, it might be expected that this application would be quite successful. This is especially true if the dispersion in the η determinations is low, as will be seen to be the case.

Fast effect

As defined for these calculations the fast effect, ε, is the number of neutrons leaving the fuel or slowing down below 100 keV per neutron born in fission. Because of the wide band of energies involved it is advantageous to use two energy groups. It has been shown by Carlvik and Pershagen[3] that under these conditions ε is given by

$$\left.\begin{aligned}\varepsilon = 1+\frac{\mathscr{R}}{\nu}\left(\nu_f-1-\frac{\sigma_{2c}}{\sigma_{2f}}\right)-\frac{\mathscr{R}}{\nu}\left(\nu_1+\frac{\sigma_{21}}{\sigma_{2f}}\right)\frac{\sigma_{1c}}{\sigma_1}\frac{P_1'}{1-(\sigma_{11}/\sigma_1)P_1'}\\ -\frac{\nu_1\sigma_{1c}}{\nu_f\sigma_1}\frac{P_1}{1-(\sigma_{11}/\sigma_1)P_1'}\end{aligned}\right\} \quad (4\text{-}7)$$

where $$\mathscr{R} = \nu\frac{\nu_2\sigma_{2f}}{\nu_f\sigma_2}\frac{P_2}{1-[(\sigma_{22}+\nu_2\sigma_{2f})/\sigma_2]P_2'} \quad (4\text{-}8)$$

ν, ν_i, ν_f = neutrons per thermal fission, per fission in group i, and per fission in both fast groups, respectively;
P_i = collision probability in group i for the first generation of neutrons;
P_i' = collision probability in group i for the second and successive generation of neutrons;
σ_i = total cross-section in group i;
σ_{ic} = capture cross-section in group i;
σ_{ij} = cross-section for the probability that a neutron in group i will be transferred to group j after a collision;
σ_{2f} = fission cross-section in group 2, the upper energy group.

Measurements of $\mathscr{R}$, the fast to thermal fission ratio, can be used as an indication of the reliability of this method, as well as assist in the selection of uncertain cross-sections. This has been done and it is expected that the resulting fast fission factors are accurate.

To take into account the fact that the rods are present in a cluster, it is necessary to make three computations:

1. ε for the entire cluster treated as homogenized;
2. ε for a single rod in the cluster;
3. ε for the homogenized medium containing the same amount of uranium as 2.

The difference between 2 and 3 can be regarded as a correction on 1.

Resonance escape probability

To obtain a reliably computed value of the resonance escape probability in a complex heterogeneous lattice requires knowledge of the effective resonance integral and the so-called resonance disadvantage factor, d—the ratio of the resonance flux in the moderator to that in the fuel. Measurements of the former have been extensive, while the latter depends primarily on theory. The particular resonance integral measurements used here are those of Hellstrand[4] who expressed the resonance integral of U^{238} as a linear function of $\sqrt{(S_{eff}/M)}$.

The effective surface, S_{eff}, in the fuel's surface to mass ratio, S_{eff}/M, is given by

$$\left.\begin{aligned} S_{eff} = {} & \text{" rubber band " surface of cluster} + \\ & + (1 - C)\,(\text{total fuel surface} - \text{" rubber band " surface}) \end{aligned}\right\} \quad (4\text{-}9)$$

where C is the Dancoff–Ginsburg self-shielding factor.[5] This formulation takes into account the shielding of the surfaces of rods in the internal parts of the cluster by nearby rods.

The task of computing resonance escape from

$$p = \exp\left(-\frac{N_{238}\,\sigma_{er}\,V_{238}}{d\sum_i V_i(\xi\,\Sigma_s)_i}\right) \quad (4\text{-}10)$$

now merely involves the computation of d. Pershagen's method[1] was to use age theory to express d^{-1} as the sum of two functions: the first representing the component of this flux ratio due to neutrons born in the cluster, and the second representing the component due to neutrons born in other clusters.

Figure 3-17 has shown that tight clustering gives higher bucklings, especially for undermoderated lattices. This curve represented the buckling difference between two lattices identical in every respect except for the inter-rod spacing within a cluster. In undermoderated lattices resonance escape is low and resonance effects contribute to

this buckling difference. Thus a tighter clustering increases the self-shielding factor C and reduces σ_{ar} thereby. This increases p and the buckling. It should also be mentioned that the fast effect is enhanced by tight clustering.

Thermal utilization

The thermal utilization factor, f, is defined here as the ratio of thermal neutrons absorbed in the fuel, $U^{235} + U^{238}$, to the total absorption of thermal neutrons. Since

$$f = \frac{(\sum_{as\,235} V_{235} + \sum_{as\,238} V_{238})\phi_{s\,\mathrm{fuel}}}{\sum_i \sum_{as\,i} V_i \phi_{s\,i}} \tag{4-11}$$

the principal component in calculating thermal utilization is the calculation of the relative thermal fluxes. It was found sufficient to compute these ratios by a combination of two methods: the S_n method[6] was used to give the flux shape within the fuel, and diffusion theory, with a transport theory boundary condition at the fuel's surface, was used to give the flux shape in the moderator. In treating the cluster, as the central zone of this cell calculation its cross-sections were obtained from a volume and flux weighted homogenization of the fuel, clad, and internal moderator.

Migration areas

The thermal migration area was computed from

$$L^2 = \overline{D}_s / \overline{\sum}_{as} \tag{4-12}$$

where $\overline{D}_s$ and $\overline{\sum}_{as}$ are volume and flux weighted values for the thermal diffusion constant and thermal microscopic absorption cross-section respectively.

The fast migration area, or neutron age, τ, was based on a measurement of 100 cm^2 from fission energies to indium resonance, 1·44 eV. However, it was necessary to modify this for four effects:

(a) there is a probability, $\mathscr{P}$, that a neutron will be inelastically scattered by the uranium with an age of about 59 cm^2;
(b) the age from indium to the " top " of the thermal spectrum, 16 kT, must be added (kT is the characteristic energy of the thermal spectrum);
(c) a correction for resonance absorption during slowing down;
(d) elastic scattering in materials other than D_2O of volume V_M does not result in energy loss.

Therefore the age is given by

$$\tau = [100(1-\mathscr{P})+59\mathscr{P}+7{\cdot}1\ln(1{\cdot}44/kT)+3{\cdot}6\ln p]\,\frac{\sum_i V_i}{V_M} \qquad (4\text{-}13)$$

Analysis of experiments

For complete *a priori* calculation of buckling, the remaining factor in Equation (4-6), η, would be computed from its theoretical formula:

$$\eta = \frac{\eta_{235}\sum_{as\,235} V_{235}}{\sum_{as\,235} V_{235} + \sum_{as\,238} V_{238}} \qquad (4\text{-}14)$$

However, it was preferred by the AB Atomenergi group to substitute the experimental bucklings into Equation (4-6) together with the other computed lattice constants and solve for the corresponding η's. This has the advantage of giving the reactivity uncertainty of the theory and experiment since $\Delta\eta/\eta$ is a reactivity change. It also provides an average η to use with the particular methods of computation above in order to arrive at results that should agree with experiment.

Twenty of the bucklings in Chapter III were used to determine η's. The result obtained by Pershagen[1] by this process was

$$\eta = 1{\cdot}302 \pm 0{\cdot}006 \qquad (4\text{-}15)$$

where 0·006 is the average deviation among the various η's. This corresponds to a combined precision of ½ per cent reactivity in experiment and theory. It must be pointed out that this type of analysis is not to be regarded as a determination of η for natural uranium to ½ per cent accuracy. However, if it were interpreted in this sense, then the precision is more like 2 per cent, since systematic errors in the theory and the experiment probably amount to this much. In fact, Pershagen's analysis of other experiments shown in Table 4-1 gave η's ranging from 1·290 to 1·320, although the internal consistency of the η's of a given experiment were better than this.

In regard to the specific values of the individual lattice constants, these are given for similar lattices in Chapter VI for computational methods somewhat similar to those of this chapter. However, it has been seen in Fig. 3-21 that lattice No. 23 is approximately midway between lattice Nos. 57 and 58 of Saclay. Therefore, Table 4-2 gives the lattice constants of lattice No. 23 as interpolated from those calculated by the methods of Chapter VI of Girard *et al.*[10] All

constants are *a priori* except η and the resonance integral, which were chosen so that a large number of buckling experiments could be fit by the theory. It is worth noting that the value of η empirically chosen by the Saclay group to fit its experiments, 1·294, is quite close to that obtained empirically by Pershagen, 1·302.

TABLE 4-1. AVERAGE η'S OBTAINED BY ANALYSIS OF BUCKLING MEASUREMENTS IN NATURAL URANIUM–HEAVY WATER LATTICES

Fuel element	Measurement	Number of bucklings analyzed	Average η
U rods	North American Aviation exponential[6]	22	$1{\cdot}316 \pm 0{\cdot}004$
U rods and clusters	AB atomenergi exponential[7]	32	$1{\cdot}320 \pm 0{\cdot}004$
U rods and rod clusters	Chalk River,[8, 9] and Saclay[10] critical	27	$1{\cdot}303 \pm 0{\cdot}003$
UO_2 rod cluster	AB atomenergi exponential[11]	20	$1{\cdot}302 \pm 0{\cdot}006$
UO_2 rod clusters	Chalk River critical[12]	4	$1{\cdot}290 \pm 0{\cdot}003$

TABLE 4-2. CONSTANTS FOR LATTICE NO. 23 AS INTERPOLATED FROM SACLAY CALCULATIONS[10]

ϵ	1·0153
σ_{ar} in barns	10·9
p	0·9340
η	1·294
$\frac{\text{moderator flux}}{\text{fuel flux}}$	1·781
f	0·9628
k_∞	1·1814
L^2 in cm^2	197·6
τ in cm^2	126·8
B^2 in μB	
Calculated from preceding:	537
Measured by Persson:	562

The measured buckling in Table 4-2 is a little larger than that calculated. However, the reason for this can be seen in Fig. 3-21. The Scandinavian exponential gave slightly larger bucklings than obtained at Saclay. The latter were used to obtain η and σ_{ar}, the

resonance integral, of Table 4-2, and therefore bucklings calculated from them are smaller than Scandinavian values.

Maximum of buckling curves

It has already been pointed out in Chapter III that a maximum in buckling results when an optimal balance between resonance and thermal neutron parameters exists. Figure 4-1 shows in a qualitative manner how p, f and L^2 behave for typical lattices encountered here. The way these combine to maximize buckling can be seen from

$$B^2 \cong \frac{\varepsilon p \eta f - 1}{L^2 + \tau} \tag{4-16}$$

ε, η and τ are relatively insensitive to the moderator to fuel ratio. However, resonance escape probability, p, thermal utilization, f, and thermal migration area, L^2 are sensitive to this ratio. As Fig. 4-1 shows, the low value of p reduces the buckling for under-

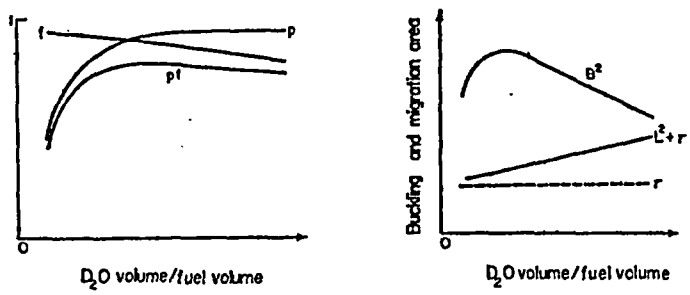

FIG. 4-1. A maximum in the buckling due to variations of p, f, and L^2 with moderator to fuel ratio.

moderated lattices, while the low f and large L^2 reduces the buckling for overmoderated lattices. Appendix C derives as an approximate formula for the buckling:

$$B^2 = -A_1 x + A_2 - A_3/x \tag{4-17}$$

A_1, A_2 and A_3 are constants which typically are sufficiently slowly varying with x, the heavy water to fuel ratio, that the location of the maximum may be had from

$$\frac{dB^2}{dx} = -A_1 + A_3/x^2 = 0 \tag{4-18}$$

Temperature coefficient

The theoretical computation of a temperature coefficient of buckling can be based on a differentiation of Equation (4-6).

$$\left.\begin{aligned}&\left(\frac{1}{\varepsilon}\frac{d\varepsilon}{dT}+\frac{1}{\eta}\frac{d\eta}{dT}+\frac{1}{p}\frac{dp}{dT}+\frac{1}{f}\frac{df}{dT}\right)k_\infty\\&=\left(B^2\frac{d\tau}{dT}+\tau\frac{dB^2}{dT}+\frac{B^2}{1+L^2B^2}\frac{dL^2}{dT}+\frac{L^2}{1+L^2B^2}\frac{dB^2}{dT}\right)\\&\qquad\qquad e^{\tau B^2}(1+L^2B^2)\end{aligned}\right\}\quad(4\text{-}19)$$

or

$$\left.\begin{aligned}\frac{dB^2}{dT}=&\left(\frac{1}{\varepsilon}\frac{d\varepsilon}{dT}+\frac{1}{\eta}\frac{d\eta}{dT}+\frac{1}{p}\frac{dp}{dT}+\frac{1}{f}\frac{df}{dT}-B^2\frac{d\tau}{dT}-\right.\\&\left.-\frac{B^2}{1+L^2B^2}\frac{dL^2}{dT}\right)\Bigg/\left(\tau+\frac{L^2}{1+L^2B^2}\right)\end{aligned}\right\}\quad(4\text{-}20)$$

The temperature coefficient of buckling here is the algebraic sum of contributions from the temperature coefficients of the six lattice constants.

The total temperature derivative d/dT in these equations can be viewed as being composed of three partial derivatives:

$$\partial/\partial T_n,\ (d\rho_{D_2O}/dT)\partial/\partial\rho_{D_2O},\ \text{and}\ \partial/\partial T_f$$

The effective neutron temperature, T_n, is determined by the shape of the thermal spectrum as well as the physical temperature of the heavy water, T. In the experiments discussed here the fuel temperature, T_f, is equal to T.

Table 4-3 gives the algebraic sign of each contributing effect.

TABLE 4-3. THE PRINCIPAL SOURCES AND SIGNS OF EFFECTS CONTRIBUTING TO THE TEMPERATURE COEFFICIENT OF BUCKLING

	from T_n	from ρ_{D_2O}	from T_f	Total
$d\varepsilon/dT$		+		+
$d\eta/dT$	−			−
dp/dT		−	−	−
df/dT	+	+		+
$-d\tau/dT$		−		−
$-dL^2/dT$	−	−		−
dB^2/dT				−

These may be verified by examination of the ways in which the neutron temperature, the heavy water density, and the fuel temperature enter into the formulae for the lattice constants. The positive coefficient in ε stems from the reduced density between the clustered rods. η's negative effect is due to the thermal absorption cross-section of U^{235} in Equation (4-14) decreasing more rapidly than that of U^{238}, with increasing T_n. A decrease in ρ_{D_2O} is responsible for the negative effects of p, τ and L^2 (although the effect can be positive for p if the Dancoff correction dominates). In addition, doppler broadening of σ_{ar} by an increasing T_f reduces p. Since the ratio of moderator to fuel flux is reduced as the moderator temperature increases, the thermal utilization is increased. Finally, another effect increasing L^2 as T_n increases stems from $\overline{\Sigma}_a$ being reduced.

The negative effects dominate the positive, and, as found experimentally in Fig. 3-18, the overall effect is a negative temperature coefficient of buckling. In the case of heavy water alone, a numerical value for the temperature coefficient of buckling is readily had from its theoretical formula in the form,

$$L^2 = \frac{L_0^2 \rho_{0\,D_2O}^2}{\rho_{D_2O}^2} \sqrt{\frac{T_n}{T_{0n}}} \tag{4-21}$$

where the subscript, zero, refers to a reference room temperature value.

$$\left.\begin{aligned} \frac{dB^2}{dT} &= \frac{1}{L^4}\frac{dL^2}{dT} \\ &= \frac{1}{L^4}\left(\frac{d\rho_{D_2O}}{dT}\frac{\partial L^2}{\partial \rho_{D_2O}} + \frac{\partial L^2}{\partial T_n}\right) \\ &= \frac{1}{L^2}\left(-\frac{2}{\rho_{D_2O}}\frac{d\rho_{D_2O}}{dT} + \frac{1}{2T_n}\right) \end{aligned}\right\} \tag{4-22}$$

This expression was evaluated for $L^2 = 8700\,\text{cm}^2$ (within the measured range of L^2 for the Scandinavian exponential) in Fig. 3-18, and is seen to compare favorably with experiment.

REFERENCES

1. B. Pershagen, G. Anderson, F. I. Carlvik, Calculation of lattice parameters for uranium rod clusters in heavy water and correlation with experiments, P/151. Geneva conference (1958).

2. N. HIDLE and O. DAHL, The Halder boiling heavy water reactor, P/559. Geneva conference (1958).
3. I. CARLVIK and B. PERSHAGEN, The fast fission effect in a cylindrical fuel element, AEF-70, AB Atomenergi, Stockholm, Sweden (1956).
4. E. HELLSTRAND, Measurements of the effective resonance integral in uranium metal and oxide in different geometries, *J. Appl. Phys.* 28, 1493 (1957).
5. S. M. DANCOFF and M. GINSBURG, Surface resonance absorption in a close-packed lattice, CP-2157 (1944).
6. E. R. COHEN, Exponential experiments on D_2O-uranium lattices, P/605. Geneva conference (1955).
7. R. PERSSON *et al.*, Exponential pile experiments with natural uranium and heavy water, *J. Nucl. Engng.* 3, 188 (1956).
8. E. CRITOPH and A. G. WARD, Comparison of theory and experiment for lattice properties of D_2O–U reactors, AECL-350 (CRRP-655), Chalk River (1956).
9. A. OKAZAKI and D. W. HONE, Lattice experiments for clusters of nineteen 1·31 cm diameter uranium metal rods in heavy water, UK/C-6/120, Chalk River (1957).
10. Y. GIRARD *et al.*, Natural uranium–heavy water lattices, experiment and theory, P/336. Geneva conference (1958).
11. R. PERSSON *et al.*, Exponential experiments on heavy water natural uranium metal and oxide lattices, P/160. Geneva conference (1958).
12. R. E. GREEN, Lattice experiments with 19-element UO_2 rods in ZEEP, UK/C-6/109, Chalk River (1957).

CHAPTER V

SACLAY $UO_2 - D_2O$ LATTICE EXPERIMENTS

Facility

The effort of France in the area of oxide – heavy water lattices took place at the Saclay Center for Nuclear Studies.[1] Here the zero power reactor, named Aquilon, was constructed. It is a heavy water critical assembly using uranium metal and oxide fuels. The motivation for this facility was the desire to make an extensive study of natural uranium heavy water lattices. The Aquilon went critical for the first time in August 1956. From that date to April 1958 the lattice studies reported here were conducted. In addition, studies involving natural uranium metal, heavy water moderated lattices were also made.

The buckling measuring technique chosen by the Saclay group was of the two region critical type, where the critical water heights rather than flux distributions were largely used as a measure of buckling. This technique is quite rapid and lends itself particularly well to small buckling changes from the buckling of the outer annular lattice. This experiment also has the advantage of requiring a relatively small amount of fuel.

A view of the Aquilon is shown in Figs. 5-1 and 5-2. A central zone of 24 elements can be seen, surrounded by the reference lattice in a square pattern in Fig. 5-2. The aluminum vessel is 280 cm high and 200 cm inside diameter, with a 0·6 cm thick side wall and 1 cm thick bottom. A graphite reflector surrounds the perifery and bottom of the vessel. Cadmium control blades move between the reflector and the tank to minimize the effect on the lattice flux and make possible "bare" cores. Safety rods, also of cadmium, capable of being dropped into the center of the reactor were also present.

Fuel handling was readily possible through holes in the reactor's rotating top cover shown in these figures. A simple crane above the reactor moved the elements which were suspended from beams across the top of the tank. Inasmuch as only 20 to 30 per cent of a critical mass was the most ever present in the central zone, lattice

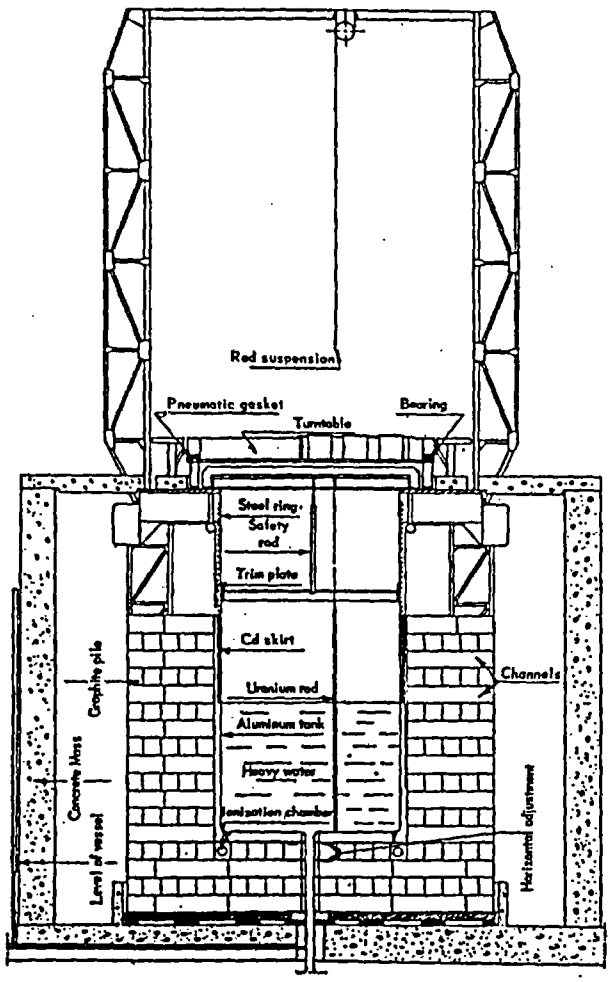

FIG. 5-1. Vertical cross-section of the Aquilon reactor.

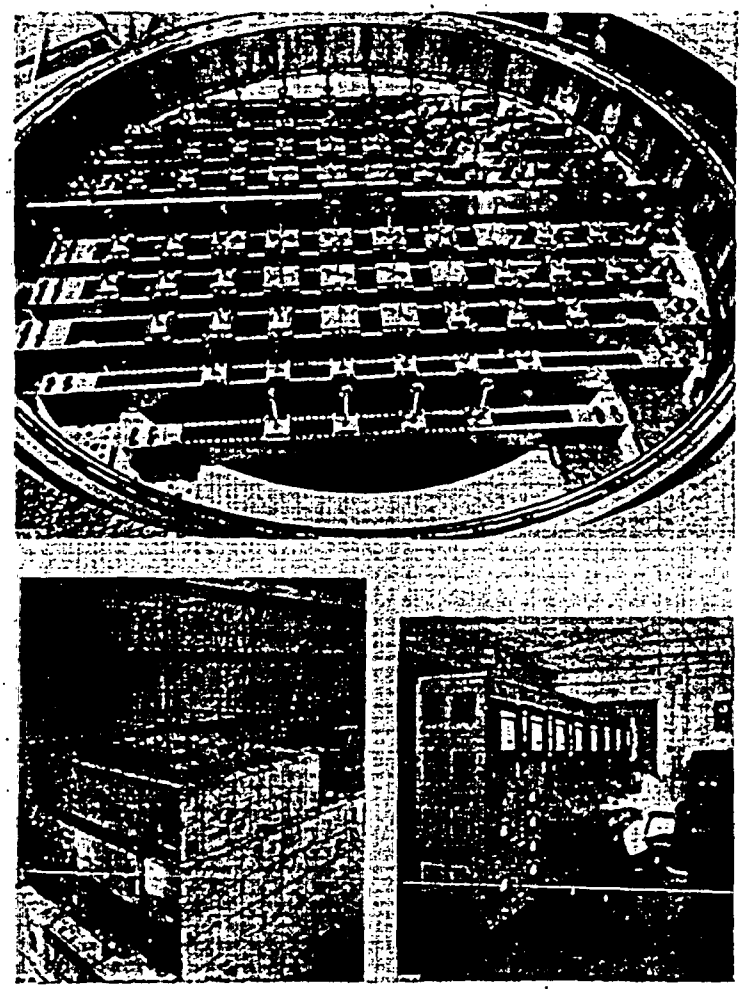

FIG. 5-2. Views of the reactor tank, the reactor room, and the control room.

changes were rapid and a buckling could be measured every 1 or 2 days.

Substitution method

The experimental technique of measuring bucklings by the two region critical, or substitution method is straightforward. A reference lattice is selected for the outer zone. It is advantageous that it resemble the lattices to be measured in the central zone. If such is the case, analysis of the experiment can be simple and precise. In particular it is advantageous for the buckling of the outer zone to be near that of the central zone. Since the experiment measures a buckling difference (see Equation 2-25), errors in measuring this difference would in such cases have little importance, and the central zone's buckling is known as accurately as that of the outer zone. However, if this buckling difference is measured precisely, this in itself is also useful information.

The Saclay group chose reference lattices from those in Table 5-1. In particular the spacing between fuel elements was chosen as that

TABLE 5-1. CHARACTERISTICS OF THE NATURAL URANIUM METAL ELEMENTS USED IN THE SACLAY REFERENCE LATTICES

	Element A	*Element B*
O.D. of Uranium metal	3·56 cm	4·4 cm
I.D. of clad	3·68 cm	4·5 cm
Thickness of clad	0·08 cm	0·1 cm
No. of rods per cluster	1	1
Buckling for square pitches of:		
15 cm	836 μB	
17 cm	786 μB	
19 cm	716 μB	
21 cm	638 μB	731 μB
23 cm	558 μB	659 μB
25 cm		587 μB

to be used in the unknown lattice. As a first step the buckling of the reference lattice was measured by loading the entire reactor with it. This involved from about 52 to 88 fuel elements. Manganese foils located in 1 cm diameter aluminum cans in the reactor were irradiated to a value of $\int\phi\, dt \cong 10^9$ neutrons per cm^2 in about 1 min. After the counting of these foils, the data were corrected and processed by an electronic computer for the buckling:

$$B^2 = B_r^2 + B_z^2 \tag{5-1}$$

The process of determining B_r^2 and B_z^2 from

$$\phi = AJ_0(B_r r)\sin B_z z \tag{5-2}$$

is quite analogous to that involved in exponential assemblies.

The replacement of the reference lattice fuel elements by the fuel elements to be investigated took place in steps: 1, 4, 12, 16, and possibly 24 clusters would successively be the cumulative member of central substitutions made. After each substitution the reactor was made critical. The critical water height was compared in each case with that of the reference lattice. The result, ΔB_z^2, was proportional to the desired buckling difference between the test and reference lattice. Details of analysis are given later in this chapter.

Lattice geometry

The Saclay experiment used five categories of fuel elements:

(a) Clusters of 7, 12 and 19 UO_2 rods 1·62 cm in diameter, shown in Figs. 5-3 and 5-4;
(b) Clusters of 13 and 19 UO_2 rods 1·56 cm in diameter from AB Atomenergie of Sweden, shown in Fig. 3-4 (however, the Saclay experiment used no shroud);
(c) Clusters of 13 and 19 UO_2 rods 1·32 cm in diameter from A.E.C.L. of Canada, shown in Figs. 5-5 and 5-6.
(d) Single UO_2 rods 3·00 cm in diameter;
(e) Single UO_2 rods 7·60 cm in diameter.

In case (b) the UO_2 rods and the inside diameter of the clad are reported as having the same dimensions.[3] (For consistency the dimensions given here are those determined by the Scandinavian group, as there is no significant difference with Saclay's determination of dimensions.) However, in the other cases it can be seen from Table 5-2 that a 0·04 or 0·05 cm air gap existed between the rod and the inside surface of the clad. The linear densities of Table 5-2 correspond to 9·85, 9·52, 9·95 and 9·95 gm/cm^3 as the mass per unit geometric volume of UO_2 for cases (a), (c), (d) and (e) respectively.

Thirty-six lattices of square spacings between clusters of 15 to 25 cm were constructed. The volume fractions and ratios of these lattices are given in Table 5-3. Here the basic lattice cell is a square of area equal to the fuel element spacing squared. One such cell has a complete cluster at its center.

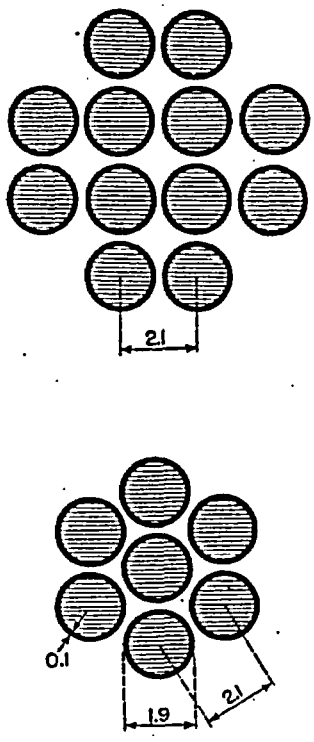

FIG. 5-3. Seven and twelve rod clusters used in lattices 54 and 55 of Saclay.

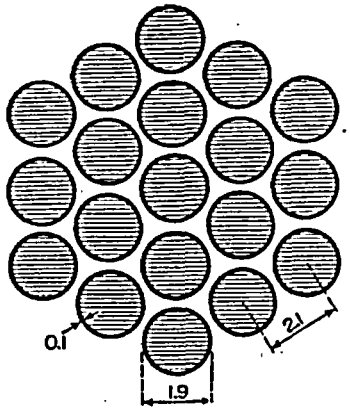

FIG. 5-4. Nineteen rod cluster used in lattice 56 of Saclay.

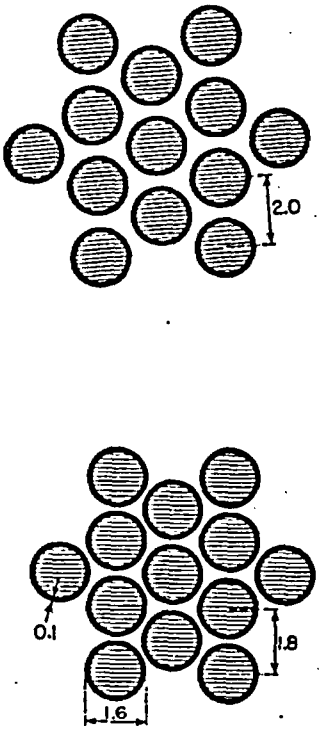

FIG. 5-5. Thirteen rod clusters used in lattices 62 through 66 of Saclay.

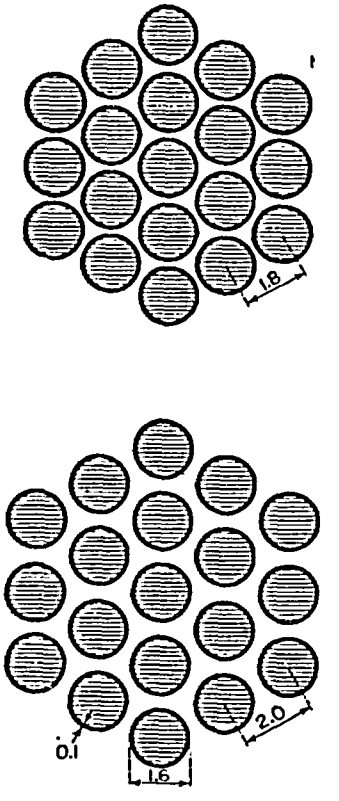

FIG. 5-6. Nineteen rod clusters used in lattices 67 through 71 of Saclay.

TABLE 5-2. DIMENSIONS OF THE SACLAY LATTICES

Lattice No.	O.D. of UO_2 in cm²	I.D. of clad in cm	Thickness of clad in cm	Grams of UO_2 per cm	Number of rods	Spacing of rods in cm	Spacing of fuel elements in cm
54a	1·62	1·7	0·1	20·3	7	2·1*	15
54b							17
54c							19
54d							21
54							23
55a					12	2·1	17
55b							19
55c							21
55							23
55d							25
56a					19	2·1*	19
56b							21
56							23
56c							25
57	1·56	1·56	0·08	18	13	1·85*	21
58							23
59					19	1·85*	21
60							23
61							25
62	1·32	1·4	0·1	13·03	13	1·8*	19
63							21
64							23
65					13	2·0*	19
66							23
67					19	1·8*	19
68							21
69							23
70					19	2·0*	19
71							23
71a	3·00	3·10	0·1	70·3	1		15
71b							17
71c							19
71d	4·60	4·70	0·1	166·2	1		15
71e							17
71f							19
71g							21

* These are hexagonal spacings. All other rod and fuel element spacings in this table are square.

TABLE 5-3. VOLUMES AND BUCKLINGS OF THE SACLAY LATTICES

Lattice No.	Volume in cm³ in a lattice cell 1 cm high			D_2O volume ÷ Fuel space*	Al volume ÷ Fuel space*	B^2 in μB
	Fuel space*	Clad	D_2O			
54a			205·2	12·93		558
54b			269·2	16·96		562
54c	15·89	3·958	341·2	21·48		536
54d			421·2	26·52		491
54			509·3	32·06		439
55a			255·0	9·37	0·2491	459
55b			327·0	12·00		539
55c	27·24	6·786	407·0	14·94		552
55			495·2	18·18		534
55d			591·0	26·70		487
56a			307·1	7·12		380
56b	43·13	10·74	387·1	8·98		488
56			475·3	11·02		532
56c			571·1	13·24		517
57	24·85	5·358	411·0	16·54		544
58			499·0	20·08		511
59			397·0	10·93	0·2156	528
60	36·32	7·831	485·0	13·36		538
61			581·1	16·00		516
62			335·0	16·74		510
63			415·1	20·74		498
64	20·01	6·126	503·1	25·14		445
65			335·0	16·74		505
66			503·1	25·14	0·3061	446
67			322·9	11·04		487
68			403·0	13·78		504
69	29·25	8·954	491·0	16·79		495
70			322·9	11·04		468
71			491·0	16·79		493
71a			216·4	28·66		526
71b	7·55	1·01	280·4	37·17	0·1338	463
71c			352·4	46·68		385
71d			206·1	11·89		657
71e	17·35	1·51	270·1	15·57	0·0871	645
71f			342·1	19·72		604
71g			422·1	24·32		548

* The fuel space is a volume 1 cm high and bounded by the inner boundary of the clad.

Bucklings

All the bucklings were measured by determinations of changes from the bucklings of Table 5-1. Although the basic measurement is a buckling change, the results reported here add this change to the buckling of the reference lattice used. Of the five categories of fuel elements in the preceding section, all used reference lattices *A* of Table 5-1, except the fuel elements of category (b) which used reference lattices *B*.

Since in general the fast to thermal flux ratios of the central zone and the reference lattice are not equal, some refinement of the simple one group statistical weight interpretation (see Equations 2-21 to 2-25) is desirable. An extension of the one group result,

$$\Delta B^2 = \frac{1}{W_1} \Delta B_z^2 \tag{5-3}$$

used by the analysts at Saclay is

$$\Delta B^2 = \frac{1}{W_1} \Delta B_z^2 + SG \tag{5-4}$$

Here W_1 is a statistical weight of the central zone. Changes in the reflector savings of the entire reactor during the measurement are also taken into account in W_1. S is an auxiliary unknown which is taken to be a function of the characteristics of the two lattices. G is a function decreasing fairly rapidly as the number of clusters in the central zone increases. The experimental data to be analyzed consisted of values of ΔB_z^2 for various radii of the central zone. Equation 5-4 was used to find a ΔB^2 and S that best fits this ΔB_z^2 data.

Figures 5-7 to 5-12 show the bucklings, which also appear in Table 5-3. Comparison with the reference lattices' bucklings of Table 5-1 indicates that the differences measured were typically of the order of -100μB. The lowest and highest difference were -24 and -338μB. It was believed that ΔB^2 was determined to within an error due to the sum of 3 per cent of ΔB^2 and 2μB. This is typically a 5μB total error. It was felt that the 3 per cent uncertainty stems from analysis techniques, while the 2μB stems from effects such as water level determination errors. An experimental confirmation of the error estimate was made by comparing the reference lattices with each other by the substitution method. Their bucklings were independently known from flux distributions and

their buckling differences were independently known from water height differences of one region critical reactors of the same radius.

An additional error in these bucklings stems from an estimated $10\mu B$ uncertainty in the bucklings of the reference lattices as deter-

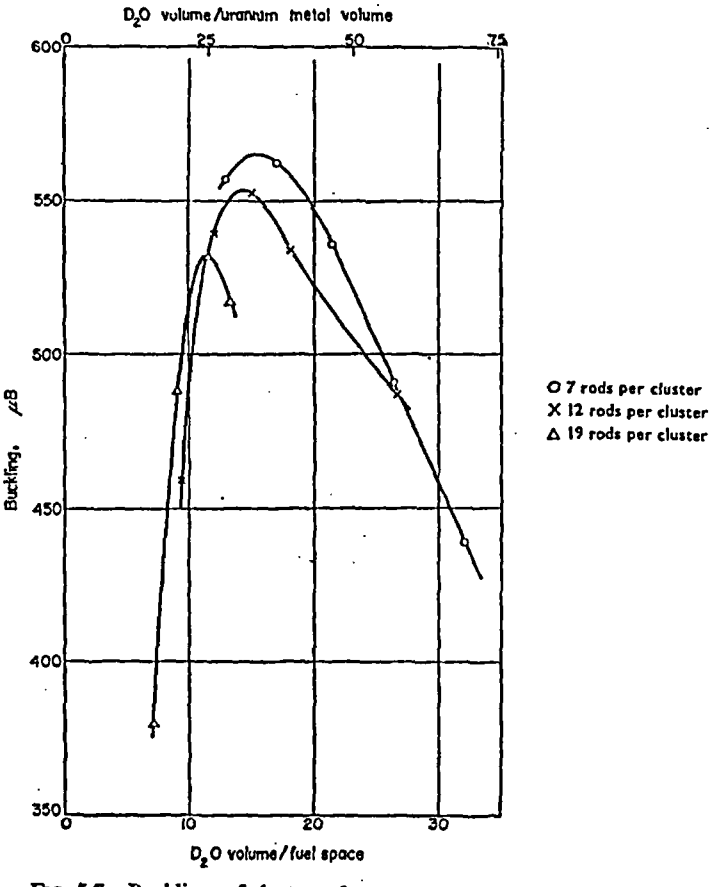

FIG. 5-7. Bucklings of clusters of seven, twelve and nineteen 1·62 cm diameter UO_2 rods (shown in Figs. 5-3 and 5-4).

mined from flux distributions. It must be pointed out that the reference lattices' bucklings used in Table 5-1 represent corrected buckling measurements. Some inconsistencies which might be observed in the inferred reflector savings have been eliminated. These corrections were never larger than $17\mu B$.

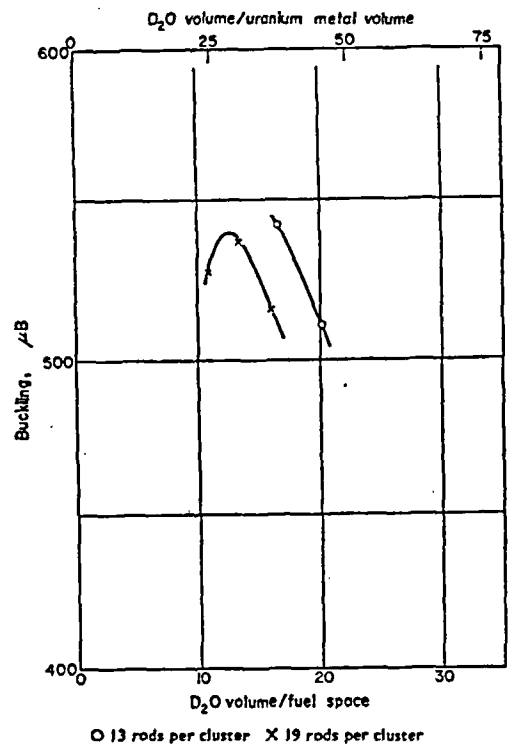

FIG. 5-8. Bucklings of clusters of thirteen and nineteen 1·56 cm diameter UO_2 rods (shown in Fig. 3-4 less shroud).

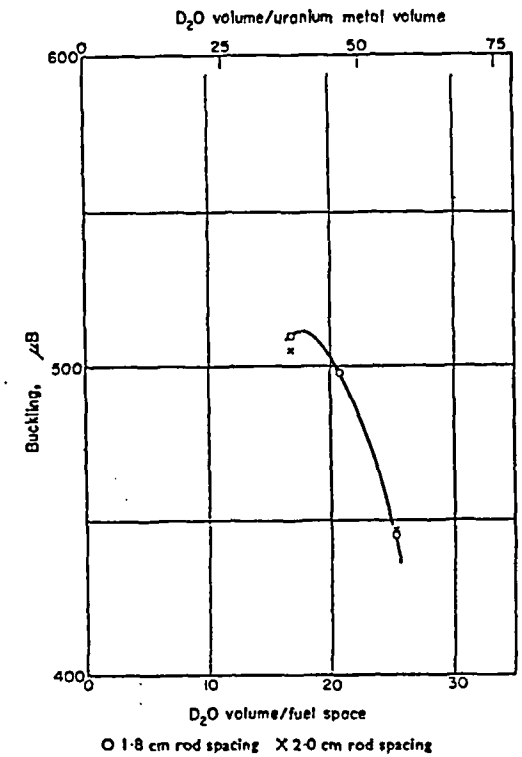

FIG. 5-9. Bucklings of clusters of thirteen 1·32 cm diameter UO_2 rods (shown in Fig. 5-5).

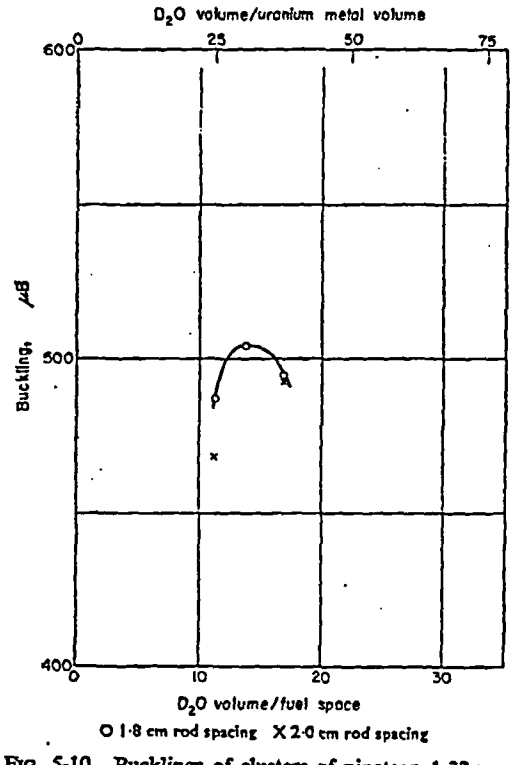

FIG. 5-10. Bucklings of clusters of nineteen 1·32 cm diameter UO_2 rods (shown in Fig. 5-6).

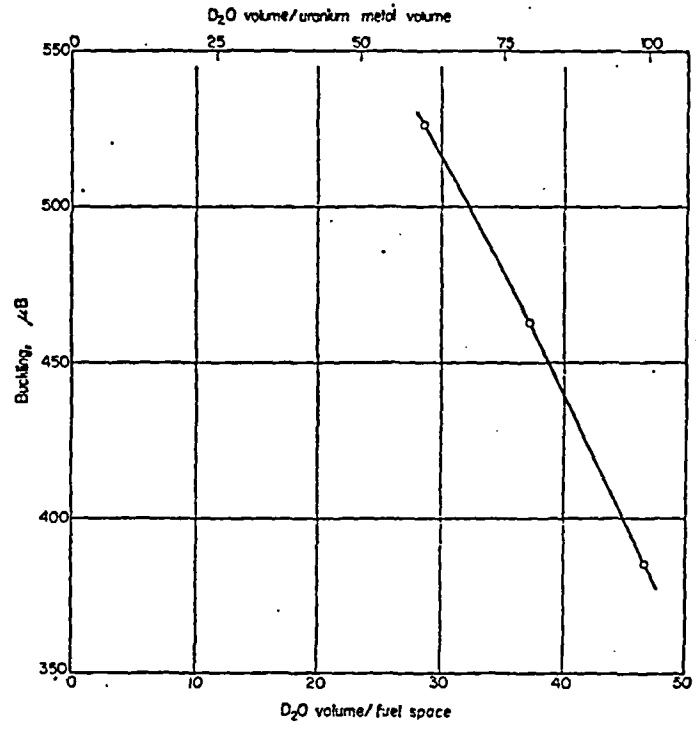

FIG. 5-11. Bucklings of single 3·00 cm diameter UO_2 rods.

Figure 5-13 shows the same effect of rod spacing within a cluster already observed in Chapter III. The tighter spacings have a higher buckling, especially at undermoderated conditions.

During this series of buckling measurements, the heavy water purity decreased from 99·82 to 99·65 per cent. By calculations of the effect of changes in the lattice constants on buckling it was possible to correct all bucklings to 99·8 per cent purity.

Discussion

The lattice substitution method of determining bucklings proved to be quite satisfactory. By being able to measure bucklings to within 15μB without the time consuming counting involved in ordinary exponentials, it competes favorably with the latter as an experimental tool. Advantages of the substitution method are:

(a) Axial buckling determinations by water height are easier than by flux distributions.
(b) An adequate flux is available for any lattice experiments requiring it if desired.
(c) Small buckling differences are easily obtained.

Disadvantages in comparison to ordinary exponentials are:

(a) Analysis and corrections can be more complex.
(b) A critical system is rather expensive, more hazardous, and requires a larger staff.

Confidence in the substitution method was obtained here in two ways. An internal consistency check indicated that lattices measured by the substitution method gave bucklings in agreement with those measured in one zone criticals. Also buckling differences as measured by lattice substitution and by one zone criticals agreed well.

A second confirmation of the results here is had by comparison of the bucklings with those obtained elsewhere by other methods using the same fuel. This was possible here since the majority of the lattices used either Scandinavian or Canadian fuel elements. Already Fig. 3-21 compared square lattices 57 and 58 of Saclay with hexagonal lattices 21, 22 and 23 of the Scandinavian exponential involving the same clusters. This systematic difference has also been observed in uranium metal lattices. The former were seen to be about 35μB smaller, and a possible explanation stemming from anisotrophy has been put forth.

Saclay lattices 67, 68 and 69 correspond to NPD-I oxide lattices measured by the Chalk River group in the ZEEP critical assembly.[2] Again the latter's hexagonal arrangement of clusters must be compared with Saclay's square arrangement having the same heavy water to fuel ratio. Fig. 5-14 shows the five bucklings from flux

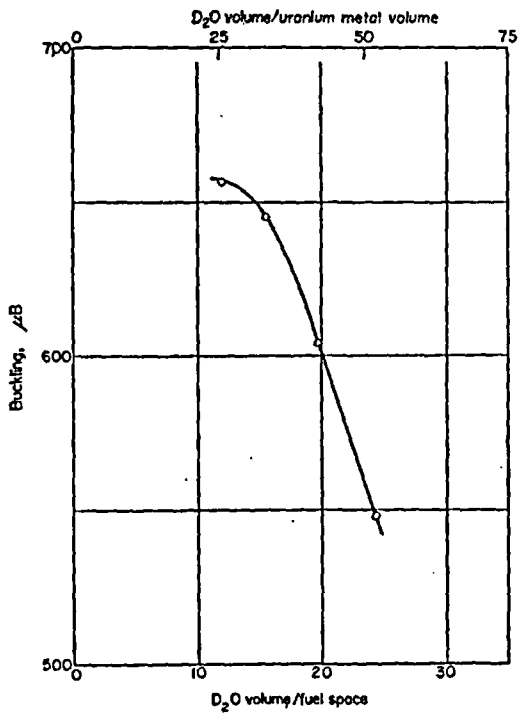

FIG. 5-12. Bucklings of single 4·60 cm diameter UO_2 rods.

distributions in the ZEEP lattices. These are corrected to 99·8 per cent purity. Here the Saclay bucklings are about 20μB lower. The agreement can be considered quite good, since the errors indicated on Fig. 5-14 do not include estimates of 10μB and 15μB systematic errors for the Saclay and Chalk River experiments respectively.

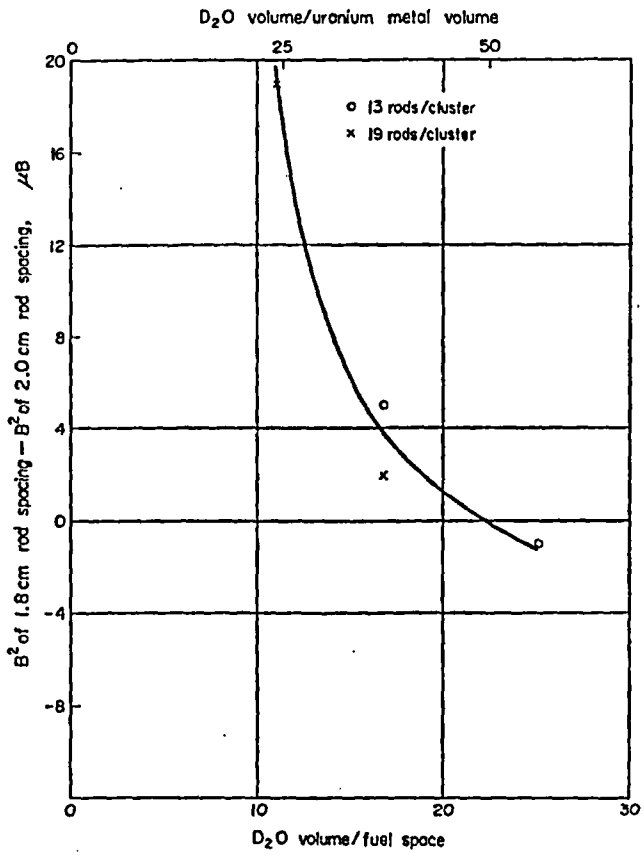

FIG. 5-13. Buckling difference between lattices of 1·8 cm and 2·0 cm rod spacings.

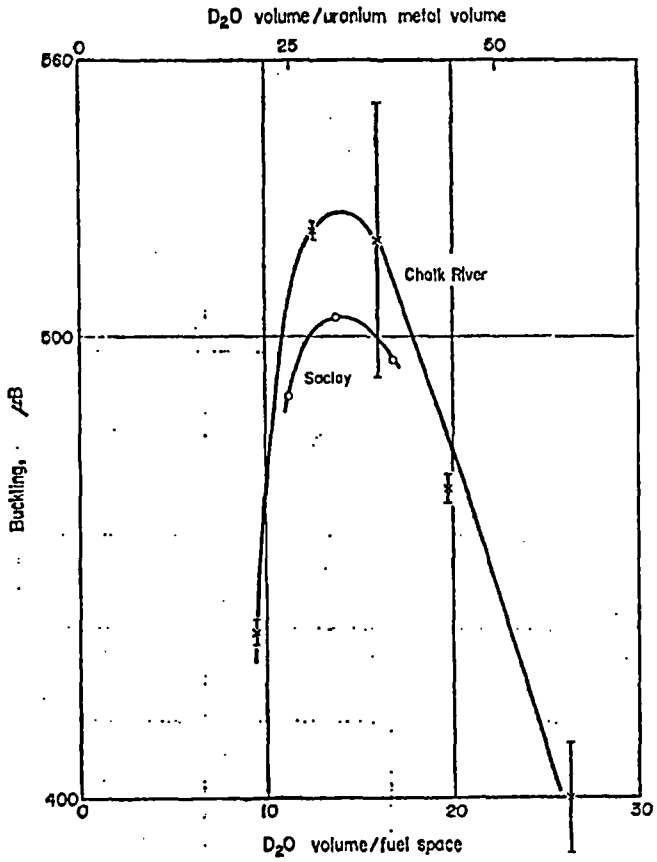

FIG. 5-14. Comparison of Chalk River and Saclay buckling measurements of the same nineteen rod cluster (Fig. 5-6).

REFERENCES

1. Y. GIRARD *et al.*, Natural uranium – heavy water lattices, P/336. Geneva conference (1958).
2. D. W. HONE *et al.*, Natural uranium – heavy water lattices, experiment and theory, P/212. Geneva conference (1958).
3. E. ANDERSEN and O. ASPELUND, Exponential experiments with uranium oxide clusters in heavy water, P/575. Geneva conference (1958).

CHAPTER VI

INTERPRETATION OF SACLAY UO_2-D_2O LATTICE EXPERIMENTS

Introduction

It has already been noted in Chapter V that the Saclay lattices included some investigated by the Scandinavian group as well as some investigated at Chalk River. The theoretical methods used by the former have already been presented in Chapter IV. Therefore, the methods used at both Saclay and Chalk River in the interpretation of these experiments will be given below. It should be borne in mind that both groups surveyed uranium metal lattices as well as those of uranium oxide. Therefore, the theoretical interpretation of the latter is somewhat colored by the presence of data from the former. This tends to add credence to the final results because of the weight of additional data brought to bear on the testing of the theory. However, only the oxide lattices are discussed here.

In the analysis of experiments both the Saclay and Chalk River groups recognized that an adjustable parameter is useful in the theory. The former allowed both η and the resonance integral to be determined by the bucklings. The Chalk River analysis used a theoretical value for η, but retained empiricism in the resonance integral. This was the effective energy of resonance capture. Also the Chalk River group was assisted in the analysis by measurements of individual lattice constants in their critical assembly.

Again the use of a particular set of theoretical methods to interpret an experiment must be viewed with the proper perspective. The resulting determinations of the adjustable parameters in the theory can hardly be viewed as direct measurements of these parameters. Rather the extent to which many bucklings can be fit by just one or two parameters is a test of the consistency of the theory used. If, moreover, the parameters so determined are in agreement with their evaluation by independent methods, then this adds additional credence to the calculational methods used.

The critical equation used in this chapter is the same as Equation

(2-5):

$$k_\infty = \varepsilon\eta p f = (1+L^2B^2)(1+\tau B^2) \tag{6-1}$$

In its derivation it has been shown to come from two diffusion theory equations, one for each group, namely Equation (2-1) and (2-2). On the other hand, the analysis by the Scandinavian group in the preceding chapter was based on age-diffusion theory. The critical equation of the latter, Equation (4-6), if τB^2 is small, does not differ significantly from Equation (6-1) since $\exp(\tau B^2) \cong 1+\tau B^2$. In later chapters, a combination of these methods of treating the fast group will be used.

Fast effect

The method of computing the fast effect used by Girard *et al.* at Saclay[1] resembles that of Chapter IV, and also takes into account a proper apportioning of neutron captures between ε and p according to Spinrad.[2] Retaining the notation of Equation (4-7), the expression for ε used is

$$\left.\begin{aligned}\varepsilon = 1 + \frac{\mathscr{R}}{\nu}(\nu_f - 1 - \sigma_{2c}/\sigma_{2f}) - \\ - \frac{(\mathscr{R}/\nu)(\nu_1+\sigma_{21}/\sigma_{2f})\sigma_{1c}/\sigma_1}{1-[(\sigma_{22}+\nu_2\sigma_{2f})/\sigma_2]P_2}\,\frac{P_1}{1-[(\sigma_1-\sigma_{1c})/\sigma_1]P_1} - \\ - \frac{\nu_1\sigma_{1c}}{\nu_f\sigma_1}\,\frac{P_1}{1-[(\sigma_1-\sigma_{1c})/\sigma_1]P_1}\end{aligned}\right\} \tag{6-2}$$

where

$$\mathscr{R} = \nu\frac{\nu_2\sigma_{2f}}{\nu_f\sigma_2}\,\frac{P_2}{1-[(\sigma_{22}+\nu_2\sigma_{2f})/\sigma_2]P_2} \tag{6-3}$$

Table 6-1 contains the cross-sections used in these equations. Some care was necessary in choosing the heavy water cross-sections that would be appropriate for use in the homogenized model for a rod cluster. The technique for homogenization must likewise be chosen with care. On the one hand, the rods at the boundary of the cluster have less opportunity for taking advantage of the compactness of the cluster. The homogeneous approximation over-estimates their fast fission. On the other hand, the interior rods by virtue of their finite size have contributions to ε which are ignored in the homogeneous approximation. It was found that by selecting the outer boundary of the cluster to be a "rubber-band" surface touching the outer oxide rods, the homogeneous approximation works best. In the homogenization process the microscopic cross-

TABLE 6-1. CROSS-SECTIONS USED IN THE CALCULATIONS OF THE FAST FISSION FACTOR

	Saclay value in *barns*	Chalk River value in *barns*
For U:		
σ_{22}	4·62	4·63
σ_{21}	2·10	2·14
σ_{2f}	0·532	0·53
σ_{2c}	0·05	0
σ_2	7·3	7·3
σ_{1c}	0·14	
σ_1	7·95	
For O:		
σ_{22}	1·97	1·97
σ_{21}	0·21	0·21
σ_{2c}	0	0
σ_2	2·18	2·18
For D_2O:		
σ_{22}	1·08	4·15
σ_{21}	1·23	2·65
ν_2/ν_f	0·561	0·551

sections, σ, in Equations (6-2) and (6-3) were replaced by macroscopic cross-sections, Σ, in all the cross-section ratios that appear, since more than one material was present.

For the fast effect computation of Hone, Critoph *et al.* at Chalk River[3] the method proposed by Spinrad[2] was again used. In terms of the fast to thermal fission ratio, $\mathscr{R}$, they obtained

$$\varepsilon = 1+0{\cdot}485\mathscr{R}\,\frac{1-\mathscr{R}[1{\cdot}0243(\sigma_{21}/\sigma_{2f})-0{\cdot}322]}{1-\mathscr{R}[0{\cdot}7245(\sigma_{21}/\sigma_{2f})-0{\cdot}429]} \qquad (6\text{-}4)$$

$\mathscr{R}$ was obtained here by Equation (6-3).

Again the cluster was treated by homogenization, but with corrections for the heterogenuities. The cross-sections used are in Table 6-1. It can be seen in Table 6-2 that the ε's computed for lattices 67 to 69 are essentially the same, whether from Equations (6-2) or (6-4). In addition measurements of $\mathscr{R}$ have confirmed these calculations in ZEEP.[3]

Figures 6-1 and 6-2 show the significant trends in the fast effect. In the former, larger values of ε result for the tighter clusters. In the latter, where this inter-rod spacing is constant, ε is larger as the rod diameter increases. In both figures as the number of rods per cluster increases, ε becomes larger. These effects are qualitatively

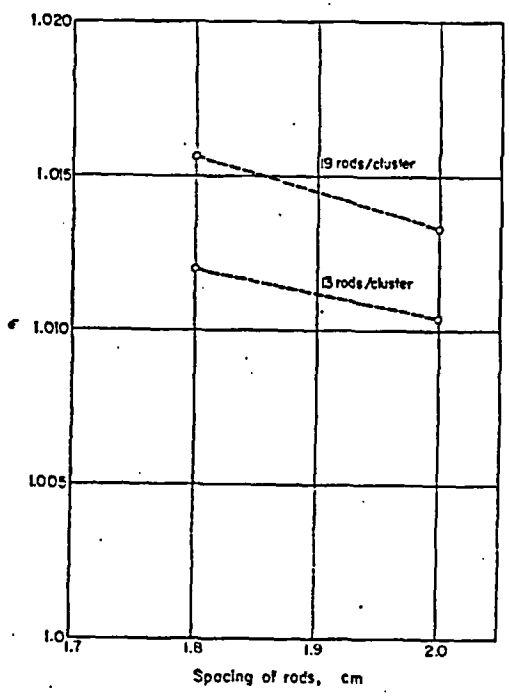

FIG. 6-1. Effect of rod spacing on the fast effect for 1·32 cm O.D. rods of lattices 62 to 71.

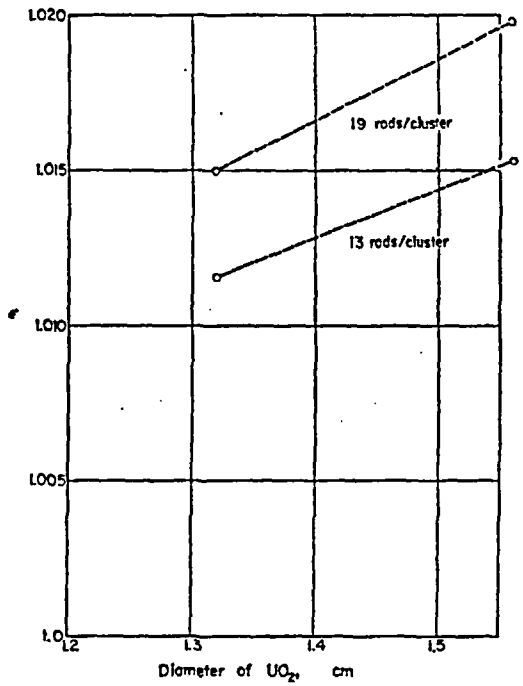

FIG. 6-2. Effect of rod diameter on the fast effect for a constant 1·85 cm spacing between rods.

TABLE 6.2. CALCULATION OF LATTICE CONSTANTS

Lattice No.	Spacing of elements		Heavy water purity	Method of calculations	ε	p	η	Moderator flux / Fuel flux	f	k_∞	L^2 in cm²	τ in cm²	B^2 in μB
	Square	Hexagonal											
54a	15		99·8%	French	1·0140	0·8883* 0·9062	1·320* 1·294	1·450	0·9649	1·1459	120·5	132·6	5·65
54b	17		,,	,,	,,	0·9093* 0·9276	1·320* 1·294	1·488	0·9817	1·1692	158·7	129·1	5·72
54c	19		,,	,,	,,	0·9239* 0·9425	1·320* 1·294	1·523	0·9580	1·1834	202·7	126·7	5·40
54d	21		,,	,,	,,	0·9343* 0·9531	1·320* 1·294	1·556	0·9540	1·1916	252·4	125·0	4·93
55a	17		,,	,,	1·0146	0·8572* 0·8744	1·320* 1·294	1·597	0·9668	1·1076	97·6	138·0	4·50
55b	19		,,	,,	,,	0·8829* 0·9006	1·320* 1·294	1·650	0·9645	1·1380	126·4	133·6	5·19
55c	21		,,	,,	,,	0·9012* 0·9193	1·320* 1·294	1·700	0·9617	1·1584	159·4	130·5	5·31
55d	25		,,	,,	,,	0·9224* 0·9409	1·320* 1·294	1·792	0·9552	1·1775	232·8	126·5	4·74
56a	19		,,	,,	1·0194	0·8287* 0·8454	1·320* 1·294	1·803	0·9679	1·0763	85·0	143·5	3·42
56b	21		,,	,,	,,	0·8581* 0·8753	1·320* 1·294	1·875	0·9660	1:1204	108·8	138·0	4·55
56c	25		,,	,,	,,	0·8915* 0·9094	1·320* 1·294	2·009	0·9612	1·1496	166·6	131·3	4·95
57	21		,,	,,	1·0153	0·9252	,,	1·750	0·9650	1·1729	171·6	128·0	555
58	23		,,	,,	,,	0·9379	,,	1·797	0·9617	1·1850	211·5	126·2	526
59	21		,,	,,	1·0198	0·8922	,,	1·894	0·9689	1·1407	125	132·6	529
60	23		,,	,,	,,	0·9108	,,	1·958	0·9664	1·1615	155·6	129·7	545
61	25		,,	,,	,,	0·9212	,,	2·017	0·9635	1·1713	190·0	127·6	519
62	19		,,	,,	1·0120	0·9292	,,	1·533	0·9534	1·1602	170·3	130·2	514
63	21		,,	,,	,,	0·9424	,,	1·570	0·9499	1·1724	212·8	127·9	487
64	23		,,	,,	,,	0·9522	,,	1·605	0·9460	1·1797	260·3	126·2	448

TABLE 6.2. CALCULATION OF LATTICE CONSTANTS—*continued*

Lattice No.	Spacing of elements		Heavy water purity	Method of calculations	ε	p	η	Moderator flux / Fuel flux	f	k_∞	L^2 in cm²	τ in cm²	B^2 in μB
	Square	Hexagonal											
65	19		,,	,,	1·0104	0·9272	,,	1·494	0·9538	1·1564	165·5	130·4	510
66	23		,,	,,	,,	0·9509	,,	1·564	0·9466	1·1769	253·1	126·4	449
67a†		19·05	99·6%	Canadian	1·0158	0·8548‡	1·3262	1·569	0·9603	1·1059	101·8	140·9	426
67	19	(20·42)	99·8%	French	1·0156	0·8971	1·2940	1·628	0·9574	1·1288	122·5	135·8	484
68a†		21·59	99·6%	Canadian	1·0158	0·8874‡	1·3262	1·626	0·9560	1·1429	136·6	136·4	507
68	21	(22·57)	99·8%	French	1·0156	0·9166	1·2940	1·678	0·9548	1·1502	154·4	132·2	506
69a†		24·13	99·6%	Canadian	1·0158	0·9080‡	1·3262	1·682	0·9511	1·1634	177·0	133·4	506
69	23	(24·72)	99·8%	French	1·0156	0·9310	1·2940	1·726	0·9518	1·1646	190·5	129·6	495
69b†		26·67	99·6%	Canadian	1·0158	0·9215‡	1·3262	1·735	0·9455	1·1738	223·0	121·4	471
70	19		99·8%	French	1·0133	0·8935	1·2940	1·571	0·9578	1·1221	117·6	136·2	467
71	23		,,	,,	1·0133	0·9285	,,	1·666	0·9524	1·1596	183·1	129·9	492
71a	15		,,	,,	1·0138	0·9390* 0·9579	1·320* 1·294	1·424	0·9655	1·2133	248·9	123·3	559
71b	17		,,	,,	,,	0·9483* 0·9674	1·320* 1·294	1·446	0·9595	1·2176	344·0	122·0	479
71c	19		,,	,,	,,	0·9547* 0·9739	1·320* 1·294	1·465	0·9526	1·2171	395·3	121·2	405
71d	15		,,	,,	1·0200	0·8892* 0·9071	1·320* 1·294	1·660	0·9802	1·1735	118·9	128·7	673
71e	17		,,	,,	,,	0·9100* 0·9283	1·320* 1·294	1·707	0·9769	1·1900	157·5	125·9	664
71f	19		,,	,,	,,	0·9244* 0·9430	1·320* 1·294	1·749	0·9732	1·2112	201·9	123·9	619
71g	21		,,	,,	,,	0·9347* 0·9535	1·320* 1·294	1·789	0·9690	1·2193	252·0	122·6	559

* Results of more recent calculations[10] after the 1958 Geneva Conference. In these η is more consistent with *a priori* methods using spectral averaging by Westcott.[11]

† The lattices, measured in ZEEP, differ from Saclay lattices only in the spacing of elements and the heavy water purity.

‡ $E_R = 25$ eV.

reasonable and can be summed up by noting that ε increases as the cluster design tends in the direction of a fast reactor design.

Resonance escape

The method of computing p used by the Saclay group was based on formulae already introduced in Chapter IV:

$$p = \exp\left(-\frac{N_{238}\,\sigma_{ar}\,V_{238}}{d\sum_i V_i(\xi\sum_s)_i}\right) \tag{6-5}$$

The resonance integral, σ_{ar}, was also taken to be a linear function of $\sqrt{(S_{eff}/M)}$, where the effective surface, S_{eff}, is the sum of an external rod surface and a Dancoff corrected internal rod surface for clusters of rods. The value which led to bucklings in closest agreement with those measured is

$$\sigma_{ar} = 5{\cdot}18 + 13{\cdot}5\sqrt{(S_{eff}/M)}\ \text{barns}^* \tag{6-6}$$

Since the Saclay analysis of the buckling experiments was based on fitting η and σ_{ar} to the data, it was deemed that detailed precise calculations of the resonance flux ratio, d, were not essential. However, the variation of d among lattices was taken into account for the larger lattice spacings. Thus the σ_{ar} that best fits the data is one to be used with d normalized to unity for the smaller lattice spacings of the experiment.

Figure 6-3 shows the values of p for the lattices of Table 6-2 having nineteen rods per cluster. The exponential dependence of p on the fuel to moderator ratio is evident. In addition it can be seen that resonance capture is enhanced by a larger rod diameter or a tighter inter-rod spacing. This is because these two effects increase σ_{ar} by increasing S_{eff}/M. The rod diameter is a direct effect, while the spacing manifests itself through the Dancoff–Ginsburg correction.

However, the method of calculating resonance escape used by Critoph[3, 4] was somewhat different. The possible need for another formulation for rod clusters was recognized when attempts at rigorous calculations of d in the historical formula, Equation (6-5), proved to be difficult. A principal feature in Critoph's method is the introduction of the concept of a single effective energy of neutrons for resonance capture, E_R. Since resonance capture in fact occurs

* Analysis[10] after the 1958 Geneva conference using all lattices from 54a to 71g, instead of just those previously published,[1] gives $6{\cdot}32 + 12{\cdot}9\sqrt{(S_{eff}/M)}$.

at many discrete energies, the use of E_R is therefore a theoretical simplification. This is somewhat analogous to a similar treatment given to the Maxwellian distribution of thermal neutrons in which a mean energy is also defined.

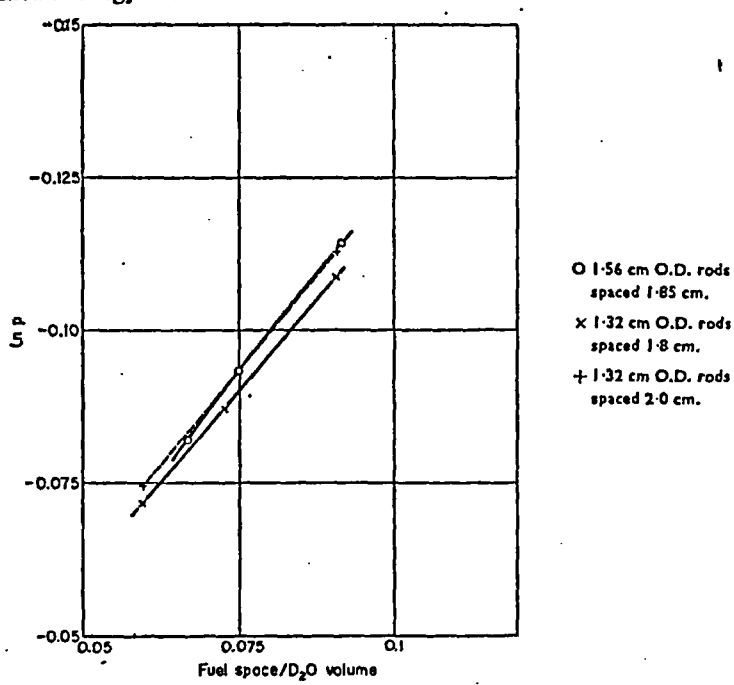

FIG. 6-3. Resonance escape for lattices 59 to 61 and 67 to 71 having nineteen rods per cluster.

For resonance capture at a single energy, E_R, by a single rod in an infinite moderating medium,

$$1-p_{0\infty} = \frac{N_{238}\,\sigma_{ar}\,V_{238}}{d\sum_i V_i(\xi\sum_s)_i} \tag{6-7}$$

The flux ratio, d, can be calculated in a straightforward fashion, assuming, for example, a slowing down density of the form,

$$\left.\begin{aligned} q(r) = \frac{0{\cdot}677}{4\pi(121-\Delta\tau)}\exp\left[-\frac{r^2/4}{121-\Delta\tau}\right] + \\ + \frac{0{\cdot}323}{4\pi(55{\cdot}6-\Delta\tau)}\exp\left[-\frac{r^2/4}{55{\cdot}6-\Delta\tau}\right]\end{aligned}\right\} \tag{6-8}$$

This is the sum of two Gaussian distribution functions of Fermi slowing down[5] from a line fission source at $r = 0$, where $\Delta\tau$ is dependent on E_R in heavy water:

$$\Delta\tau = 7{\cdot}2 \ln \frac{E_R}{1{\cdot}44\,\text{eV}} \tag{6-9}$$

Next, to obtain p_0, the probability for escape from resonance capture in a rod for a neutron born in that rod when the surrounding medium has similar rods:

$$1 - p_0 = (1 - p_{0\infty})(1 - Y)(1 - X) \tag{6-10}$$

The previous capture probability, $1 - p_{0\infty}$, is reduced by a computed escape probability for capture in neighboring rods, $1 - Y$, and corrected for changes in the surrounding medium's moderating ability by $1 - X$. Finally, to obtain p from p_0 one adds the effect of source neutrons born in neighboring rods at distances of r_i:

$$1 - p = (1 - p_0)(q(0) + \sum_i q(r_i))/q(0) \tag{6-11}$$

The σ_{ar} appearing in Equation (6-7) was based on flux depression corrected[6] resonance integral measurements,[7]

$$\sigma_{ar} = \frac{10{\cdot}1}{[\kappa_r r_f I_0(\kappa_r r_f)]/2I_1(\kappa_r r_f)} + 30{\cdot}0 \frac{S_{eff}}{M} \text{ barns} \tag{6-12}$$

where r_f is the radius of the fuel, and κ_r its inverse resonance diffusion length.

The factor, $\kappa_r r_f I_0(\kappa_r r_f)/2I_1(\kappa_r r_f)$, is the result from diffusion theory for the ratio of the surface resonance flux to the average interior resonance flux for the fuel. Rather than selecting σ_{ar} to fit the buckling measurements (as the Saclay group chose Equation 6-6), Critoph varied E_R until he found that $E_R = 25$ eV gave a best fit of theory to ZEEP experiments.

Thermal utilization

Since the formula for thermal utilization is standard,

$$f = \frac{(\sum_{as\,235} V_{235} + \sum_{as\,238} V_{238})\phi_{r\,\text{fuel}}}{\sum_i \sum_{as\,i} V_i \phi_{s\,i}} \tag{6-13}$$

only the methods of calculating the thermal flux fine structure, ϕ_s, differ among theoreticians. The Saclay group used the theory of Amouyal and Benoist,[8] which applies integral transport theory to the fuel rods and diffusion theory to the larger moderator region.

This same approach was used by the Chalk River group, although Kushneriuk[9] was followed instead. The latter uses integral transport theory to compute blacknesses for the central region.

Table 6-2 indicates virtual agreement of these methods for the calculation of moderator to fuel flux ratio, although the Amouyal method seems to have given slightly higher results than Kushneriuk's. It is also worth noting that the heavy water purity differs slightly for these two analyses.

In these lattices the dominating parasitic absorption occurred in the aluminum clad. It can be seen in Table 6-2 that the values of $1-f$ for lattices 57 to 61 range around 0·035, while lattices 62 to 71 have $1-f$ values about 50 per cent higher. This can be correlated with the aluminum volume to fuel space ratio in Table 5-3. This is 0·2156 and 0·3061 respectively for these lattice groups. Equation (6-13) indicates that $1-f$ should be proportional to this ratio, for

$$\left.\begin{aligned} 1-f &= \frac{\sum_{as\,\mathrm{Al}} V_{\mathrm{Al}}\phi_{s\,\mathrm{Al}} + \sum_{as\,M} V_M \phi_M}{\sum_i \sum_{as\,i} V_i \phi_{s\,i}} \\ &\cong \frac{\sum_{as\,\mathrm{Al}} \phi_{s\,\mathrm{Al}}}{\sum_{as\,\mathrm{fuel}} \phi_{s\,\mathrm{fuel}}} \times \frac{V_{\mathrm{Al}}}{V_{\mathrm{fuel}}} \end{aligned}\right\} \qquad (6\text{-}14)$$

Migration areas

The method of computing the thermal migration area, L^2, from

$$L^2 = \bar{D}_s / \bar{\Sigma}_{as} \qquad (6\text{-}15)$$

is primarily a matter of the technique used to calculate $\bar{D}_s$. The calculation of the average thermal absorption microscopic cross-section, $\bar{\Sigma}_{as}$, is merely a volume and flux weighed average of the $\Sigma_{as\,i}$, in the i materials. The Saclay group, as an approximation of an unpublished rigorous investigation of $\bar{D}_s$ by Benoist, used

$$\left.\begin{aligned} \frac{1}{3\bar{D}_s} = \bar{\Sigma}_{ts} = \Bigg[\left(\frac{\sum_{ts\,\mathrm{U}}^{-1} V_{\mathrm{U}}\phi_{s\,\mathrm{U}} + \sum_{ts\,M}^{-1} V_M \phi_{s\,M}}{V_{\mathrm{U}}\phi_{s\,\mathrm{U}} + V_M \phi_{s\,M}}\right)^{-1} (V_{\mathrm{U}} + V_M) + \\ + \sum_{ts\,\mathrm{Al}} V_{\mathrm{Al}}\Bigg] \Big/ (V_{\mathrm{U}} + V_M + V_{\mathrm{Al}}) \end{aligned}\right\} \qquad (6\text{-}16)$$

This is seen to represent a volume weighing of the aluminum and the uranium – heavy water mixture cross-sections. The former actually is negligible in practice. The latter in Equation (6-16) is seen to be determined by a volume and flux weighing of mean free paths.

Figure 6-4 shows L^2 to be almost linear in the moderator to fuel ratio. This is because the $\bar{\Sigma}_{as}$ in the denominator of Equation (6-15) is very nearly proportional to the fuel to moderator ratio in these lattices. The fact that L^2 is larger for the larger diameter rods and tighter rod spacings stems from the effect of the disadvantage factor on L^2.

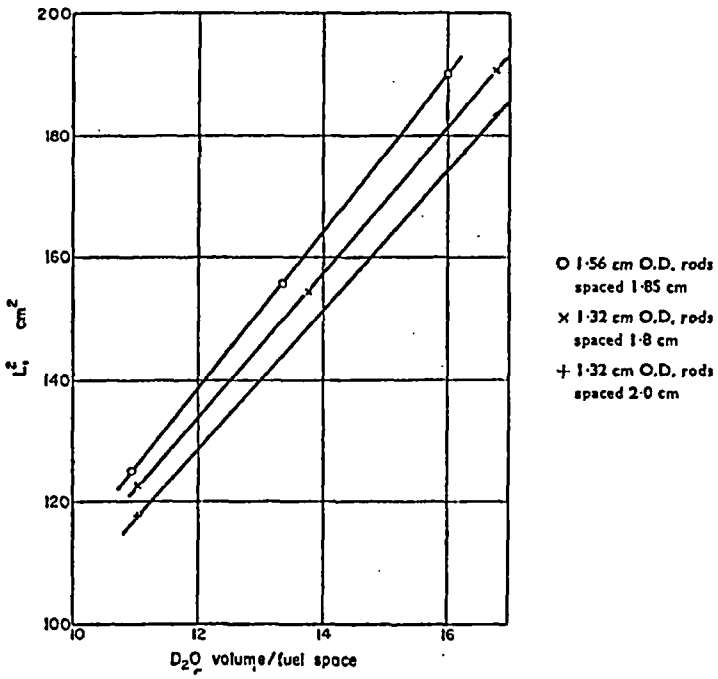

FIG. 6-4. L^2 for lattices 59 to 61 and 67 to 71 having nineteen rods per cluster.

On the other hand the method of computing $\bar{D}_s$ used in the Chalk River analysis was

$$\frac{3}{\bar{D}_s} = \bar{\Sigma}_{ts} = \left(\frac{\Sigma_{ts\mathrm{U}}^{-1} V_{\mathrm{U}} + \Sigma_{ts\mathrm{Al}}^{-1} V_{\mathrm{Al}} + \Sigma_{ts\mathrm{M}}^{-1} V_{\mathrm{M}}}{V_{\mathrm{U}} + V_{\mathrm{Al}} + V_{\mathrm{M}}}\right)^{-1} \qquad (6\text{-}17)$$

Since the uranium and heavy water cross-sections in these formulae are quite close in value, and since the volume fraction of aluminum is small, close agreement between Equations (6-16) and (6-17) can be expected, as is the case in L^2 as well.

In the age calculation, a formula somewhat similar to Equation (4-13) was used:

$$\tau = [\tau_M(1-\mathscr{P})+\tau_f\mathscr{P}]\,\frac{\sum_i V_i}{D_{fM}\sum_i V_i D_{fi}^{-1}}\,\frac{\sum_i V_i}{(\xi\sum_s)_M^{-1}\sum_i V_i(\xi\sum_s)_i} \qquad (6\text{-}18)$$

The probability, $\mathscr{P}$, that a neutron will be inelastically scattered by the uranium can be computed quite readily when the component parts of the fast effect calculation are known, τ_M and τ_F the moderator and fuel ages, were taken to be respectively 120 and 72 cm^2 at Saclay, and 125 and 103 cm^2 at Chalk River. The former also made the simplifications: the aluminum has no diffusion or slowing down; the fuel has a D_f equal to that of heavy water; the $\xi\Sigma_s$ of the fuel is taken to be zero.

The Saclay analysis of bucklings

As mentioned above, the philosophy of analysis used was to find a best fit of η and σ_{ar} to the measured bucklings. It was expected that these two parameters could be taken as constant for a given fuel element in a series of measurements in which only the spacing between fuel elements changes. That this is true of η is apparent from considerations of neutron spectra. According to Equation (4-14), η is a function of the ratio of U^{235} and U^{238} absorption cross-sections. The latter decreases with neutron energy in a $1/E$ manner, and the former almost so. The quotient of these cross-sections is therefore only slightly dependent on the mean thermal energy. The spectra in lattices studied here are virtually Maxwellian of energy 0·025 eV and change very little in nature as the lattice spacing changes. Therefore, η is a constant.

On the other hand σ_{ar} of U^{238} is a function of S_{eff}/M for the fuel element in question. However, for a given fuel element, changes in element spacings have a negligible effect of σ_{ar}. Thus one σ_{ar} can be found for each fuel element that results in a best fit to the bucklings measured at different pitches.

The method of fitting η and σ_{ar} to a set of bucklings was based on a manipulation of the critical equation, Equation (6-1):

$$\ln\eta+\ln p = \ln\frac{(1+L^2B^2)(1+\tau B^2)}{\varepsilon f} \qquad (6\text{-}19)$$

But from Equation (6-5)

$$\ln p = -\frac{N_{238}\,V_{238}}{d\sum_i V_i(\xi\sum_s)_i}\,\sigma_{ar} \tag{6-20}$$

Hence

$$\ln\frac{(1+L^2B^2)(1+\tau B^2)}{\varepsilon f} = -\frac{N_{238}\,V_{238}}{d\sum_i V_i(\xi\sum_s)_i}\,\sigma_{ar}+\ln\eta \tag{6-21}$$

Therefore, a plot of the expression on the right-hand side of Equation (6-21) against $N_{238}V_{238}/d\sum_i V_i(\xi\Sigma_s)_i$ was expected to be a straight line of slope $-\sigma_{ar}$ and intercept, $\ln\eta$. All quantities were calculated from theory except B^2 which was measured, and of course σ_{ar} and η, which were determined from the plot.

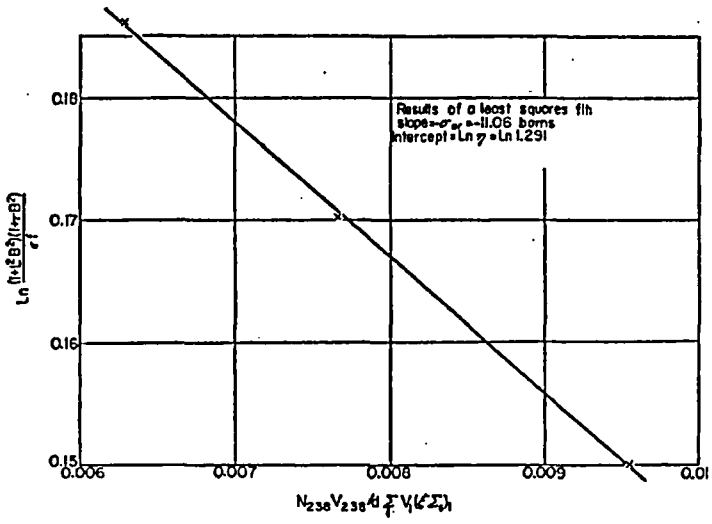

FIG. 6-5. An example of the determination of η and σ_{ar} from the measured bucklings of lattices 67, 68 and 69.

Figure 6-5 is a typical example of this type of analysis. An almost perfect linear fit is seen to be had, indicating that the relative precision of buckling measurements as well as lattice constants calculations is good. The value of η and σ_{ar} obtained in Fig. 6-5 correspond closely to the average results of determinations from the lattices 57 to 71 studied, namely:

$$\eta = 1{\cdot}294 \tag{6-22}$$

$$\sigma_{ar} = 5{\cdot}18+13{\cdot}5\sqrt{(S_{eff}/M)} \tag{6-23}$$

which for the fuel element used in Fig. 6-5 is 11·36 *barns*. If lattices 54a to 56c and 71a to 71g are incorporated into this analysis, the result for σ_{ar} is[10]

$$\sigma_{ar} = 6{\cdot}32 + 12{\cdot}9\sqrt{(S_{eff}/M)} \qquad (6\text{-}24)$$

TABLE 6-3. COMPARISON OF CALCULATED AND MEASURED BUCKLINGS

Lattice No	Calculated *buckling in μB E_R = 25eV	Calculated *buckling in μB E_R = 100eV	Measured* buckling in μB At Chalk River	Measured* buckling in μB At Saclay
54a		565		558
54b		572		562
54c		540		536
54d		493		491
55a		450		459
55b		519		539
55c		531		552
55d		474		487
56a		342		380
56b		455		488
56c		495		517
57		555		544
58		526		511
59		529		528
60		545		538
61		519		516
62		514		510
63		487		498
64		448		445
65		510		505
66		449		446
67a	441	423	436	
67		484		487
68a	526	498	523	
68		506		504
69a	527	493	521	
69		495		495
69b	493	458	467	
70		467		468
71		492		493
71a		559		526
71b		479		463
71c		405		385
71d		673		657
71e		664		645
71f		619		604
71g		559		548

* All bucklings have been corrected to a heavy water purity of 99·8%.

Lattices 57 to 71 of Table 6-2 have their bucklings calculated by the use of the theoretical formulae and methods above plus the empirically determined constants, Equations (6-22) and (6-23). The latter relationship was had by determinations of σ_{ar} for various fuel elements having various values of S_{eff}/M. Since Equations (6-22) and (6-23) were obtained by a best fit of the theory to the measured bucklings, as demonstrated by Fig. 6-5, it is expected that the calculated bucklings should agree well with the measured values. This is in fact the case in Table 6-3 for the average buckling difference of the empiracized theory and experiment is only 5μB. The other lattices (54a to 56c and 71a to 71g) have an average discrepancy of 17μB.

The Chalk River analysis of bucklings

The analytical approach used by this group was to regard the mean resonance energy, E_R, in Equation (6-9) as the parameter in the theory to be fitted to experiment. It can be seen that E_R influences $\Delta\tau$, the age from E_R to the indium resonance energy. Therefore, it affects the spatial distribution of the slowing down density, $q(r)$, in Equation (6-8). This in turn influences the value of p according to Equations (6-7) and (6-11).

Table 6-4 shows the effect of E_R on p numerically for the lattices

TABLE 6-4. EFFECT OF THE MEAN RESONANCE ENERGY ON LATTICE CONSTANTS

Lattice No	p		k_∞		B^2	
	E_R=25eV	E_R=100eV	E_R=25eV	E_R=100eV	E_R=25eV	E_R=100eV
67a	0·8548	0·8513	1·1059	1·1013	426	408
68a	0·8874	0·8808	1·1429	1·1344	507	479
69a	0·9080	0·8990	1·1634	1·1519	506	472
69b	0·9215	0·9108	1·1738	1·1609	471	436

studied. It is seen that increasing E_R from 25 to 100 eV reduces p by about 1 per cent for the larger lattice spacings. In this manner, calculating p for various E_R's, it was found that E_R = 25 eV results for the best fit to the measured bucklings in ZEEP. This obviously is not a direct measurement of the mean energy of resonance capture. Rather the meaning of the result is that this resonance energy, if used in the above method of calculation, gives bucklings in agreement with experiments in ZEEP.

However, Fig. 5-14 has shown ZEEP experiments to be about $20\mu B$ larger than those of Saclay, after correction to the same heavy water purity. If the Saclay measurements were used instead to choose the best value of E_R, it can be seen from Table 6-3 that a value slightly under 100 eV might be chosen in that case. In any event, the fact that E_R does fall approximately in the energy region where there are indeed resonances (rather than having some artificial value outside the logical range), is an indication of the self-consistency of the theory and the measurements.

It can be seen in summary that more than one self-consistent set of theoretical methods can be used to correlate the buckling data. Those presented here differ somewhat in their treatment of η and p. In fact, the η's in Table 6-2 differ by only $2\frac{1}{2}$ per cent, but, as the differences in resonance escape are in a direction opposite to this, both theories agree with measured bucklings quite well.

REFERENCES

1. Y. Girard *et al.*, Natural uranium – heavy water lattices, P/336. Geneva conference (1958).
2. B. I. Spinrad, Fast effect in lattice reactors, NSE 1, 455 (1956).
3. D. W. Hone *et al.*, Natural uranium – heavy water lattices, experiment and theory, P/212. Geneva conference (1958).
4. E. Critoph, Comparison of theory and experiment for: (a) Lattice properties of D_2O – U reactors; (b) Central rod experiments; (c) Foreign rod experiments, CRRP-655, AECL No. 350 (1956).
5. S. Glasstone and M. Edlund, *The Elements of Nuclear Reactor Theory*, p. 172. Van Nostrand, New York (1952).
6. S. Glasstone and M. Edlund, *The Elements of Nuclear Reactor Theory*, p. 272. Van Nostrand, New York (1952).
7. E. Hellstrand, Measurements of the effective resonance integral in uranium metal and oxide in different geometries, *J. Appl. Phys.* 28, 1493 (1957).
8. A. Amouyal and P. Benoist, A new method of determining the thermal utilization factor of a cell, Report CEA-571, Centre d'Etudes Nucléaires, Saclay, France (1956).
9. S. A. Kushneriuk, Neutron capture by long cylindrical bodies surrounded by predominantly scattering media, Report CRT-712, Chalk River, Ontario (1957).
10. R. Naudet, Interpretation d'un nouvel ensemble de mesures de laplaciene dans Aquilon, Report SPM–571, Centre d'Etudes Nucléaires, Saclay, France (1959).
11. C. H. Westcott, Effective cross-section values for well-moderated thermal reactor spectra, CRRP-787, Chalk River, Ontario (1958).

CHAPTER VII

SAVANNAH UO_2 – D_2O LATTICE EXPERIMENTS

Facility

Two Savannah River facilities have been used for buckling measurements: the SE (Subcritical Experiment), and the PDP (Process Development Pile). A third, the PSE (Pressurized Subcritical Experiment) was underway in 1958 and has a program of extending the low temperature data in uranium – heavy water systems to the high temperatures used in power reactors.

Most bucklings reported by Savannah River[1, 2, 3] were performed in the PDP used as a two-region critical. The bucklings were measured from water heights. As in European facilities, the fuel elements hung vertically. The ease of making these measurements allowed more than 250 lattices to be studied in a couple of years. However, only 34 are reported here, and these were measured in 1957. The other lattices were principally of uranium metal rods and plates.

The central region of the PDP allocated to lattice substitution experiments was of sufficient size to accommodate seven fuel clusters in a 7 in. hexagonal spacing, and three clusters in a 10·7 in. spacing. It might be noted that the size of this zone, about 21 in. in diameter, is somewhat smaller than the typical 40 in. × 40 in. central zone of the Aquilon. Therefore, the Savannah experiment required more careful analysis, particularly in regard to corrections stemming from resonance neutron capture effects at the boundary. However, as with the Saclay experiments, the Savannah experiments had some confirmation of the analytical methods by comparison with bucklings by other methods, such as from the SE.

Lattice geometry

Thirty-four lattices were investigated by the Savannah group using natural uranium oxide pellets provided by the Atomic Power Division of the Westinghouse Electric Corporation. These were 0·37 in. diameter pellets for all the lattices. Essentially three categories of lattices were constructed:

(a) Clusters of 13 to 61 rods, unshrouded, and having hexagonal pitches of 7 to 10·7 in. between clusters;

(b) Clusters of 19 to 37 rods having shrouded heavy water as coolant, and having hexagonal pitches of 9·26 and 10·7 in. between clusters;

(c) Clusters of 19 to 37 rods, having shrouded helium as coolant, and having hexagonal pitches of 9·26 and 10·7 in. between clusters.

TABLE 7-1. DIMENSIONS OF THE SAVANNAH LATTICES

Lattice No.	O.D. of UO_2 in in.	I.D. of clad in in.	Thickness of clad in in.	Grams of UO_2 per cm	Number of rods	Spacing of rods in in.	I.D. of shroud in in.	Thickness of shroud in in.	Spacing of fuel elements in in.
72					13				7
73					19				7
74									9·26
75					31				7
76									9·26
77									10·7
78					37	0·632	—	0	7
79									9·26
80									10·7
81					43				9·26
82									10·7
83					55				10·7
84					61				10·7
85					13				7
86					19				7
87									9·26
88	0·37	0·402	0·049	7·01	31	0·795	—	0	7
89									9·26
90									10·7
91					37				7
92									9·26
93									10·7
94					19				9·26
95									10·7
96					31				9·26
97									10·7
98					37				9·26
99						0·632	4·773	0·051	10·7
100					19				9·26
101									10·7
102					31				9·26
103									10·7
104					37				9·26
105									10·7

TABLE 7-2. VOLUMES AND BUCKLINGS OF THE SAVANNAH LATTICE

Lattice No.	Volume in in. in a lattice cell 1 in. high					D_2O volume/fuel space*	Al volume/fuel space*	B^2 in μB
	Fuel space*	Clad	Shroud	D_2O Internal	D_2O External			
72	1·65	0·9025		39·88		24·17		466
73	2·412	1·319		38·70		16·05		452
74				70·52		29·25		429
75	3·935	2·152		36·35		9·238		221
76				68·17		17·33		433
77				93·07		23·65		417
78	4·696	2·569		35·17		7·489		71
79				66·99		14·27		408
80				91·89		19·57		418
81	5·458	2·985	0	65·81		12·06		367
82				90·71		16·62	0·5470	409
83	6·981	3·818		88·35		12·66		356
84	7·742	4·235		87·18		11·26		320
85	1·65	0·9025		39·88		24·17		444
86	2·412	1·319		38·70		16·05		409
87				70·52		29·25		413
88	3·935	2·152		36·35		9·238		116
89				68·17		17·33		402
90				93·07		23·65		403
91	4·696	2·569		35·17		7·489		−94
92				66·99		14·27		356
93				91·89		19·57		395
94	2·412	1·319	0·7729	14·16	55·59	28·92	0·8673	320
95				14·16	80·48	39·24		266
96	3·935	2·152		11·81	55·59	17·12	0·7440	349
97				11·81	80·48	23·45		345
98	4·696	2·569		10·63	55·59	14·10	0·7116	334
99				10·63	80·48	19·40		343
100	2·412	1·319		0	55·59	23·04	0·8673	211
101					80·48	33·37		209
102	3·935	2·152			55·59	14·13	0·7440	240
103					80·48	20·45		280
104	4·696	2·569			55·59	11·84	0·7116	242
105					80·48	17·14		302

* The fuel space is a volume 1 in. high and branded by the inner boundary of the clad.

In addition, the first category used two spacings of rods within the clusters. It is evident that buckling data were obtained here for

both heavy water cooled and helium cooled reactors. Furthermore, these data are of value for the boiling heavy water reactor, since the latter's coolant is of a density which is between that of (b) and (c).

Tables 7-1 and 7-2 give the dimensions and volumes of these lattices. The corresponding fuel elements appear in Figs. 7-1 to 7-6. The mass per unit geometric volume of UO_2 and mass per unit internal clad volume are respectively 10·1 and 8·56 g/cm^3. This substantial difference is due to the sizeable gap between the fuel and the clad. Again the basic cell in Table 7-2 is a hexagon of area equal to 0·866 times the square of the lattice spacing.

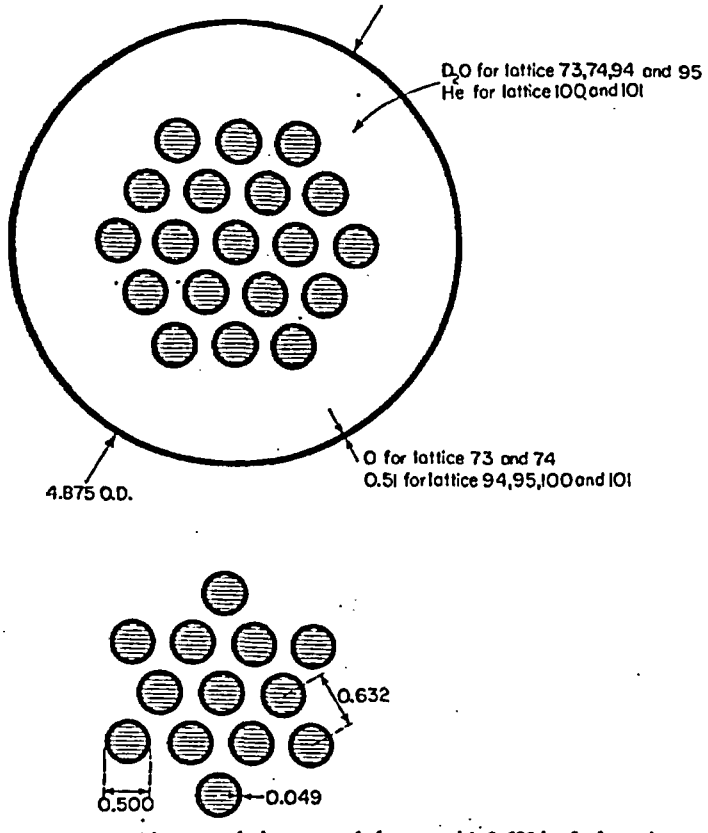

FIG. 7-1. Thirteen and nineteen rod clusters with 0·632 in. fuel spacings used in lattices 72 through 74, 94, 95, 100 and 101 of the Savannah experiments (all dimensions are in inches).

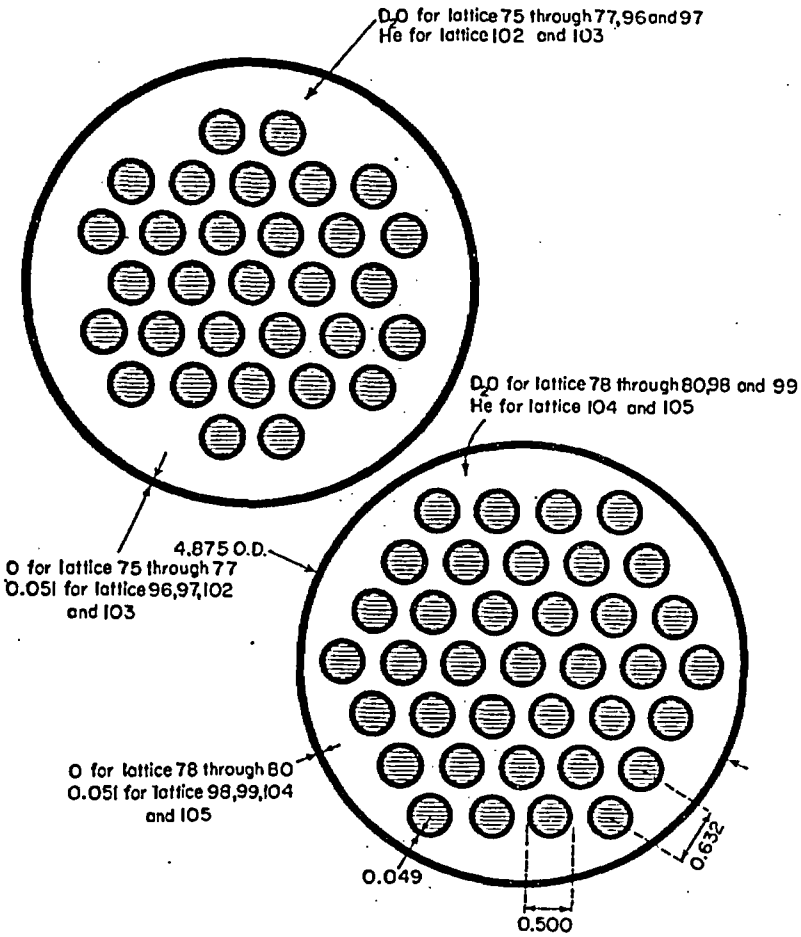

FIG. 7-2. Thirty-one and thirty-seven rod clusters with 0·632 in. fuel spacings used in lattices 75 through 80, 96 through 99, and 102 through 105 of the Savannah experiments (all dimensions are in inches).

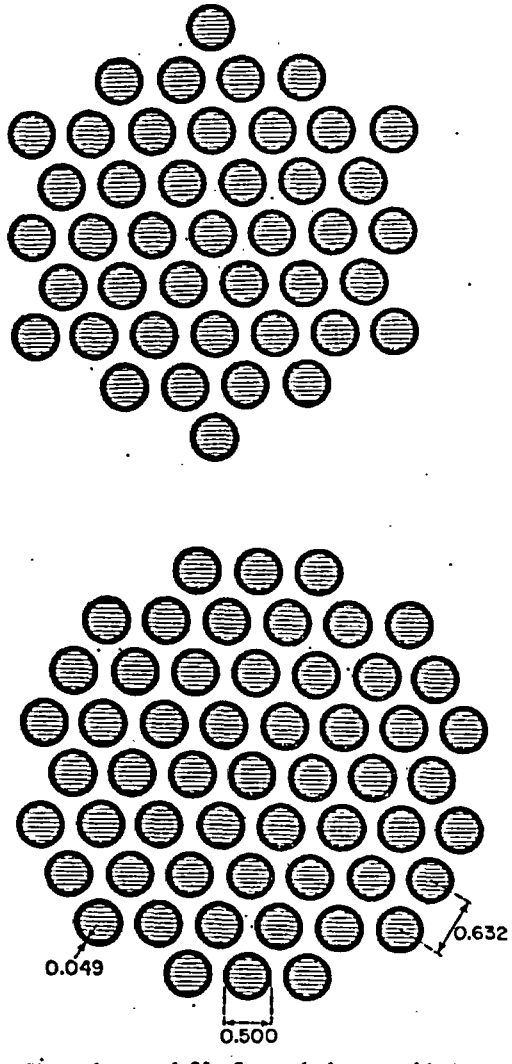

FIG. 7-3. Forty-three and fifty-five rod clusters with 0·632 in. fuel spacings used in lattices 81 through 83 of the Savannah experiments (all dimensions are in inches).

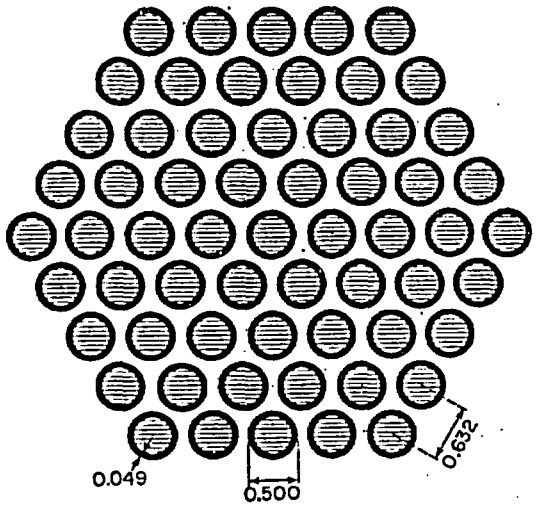

FIG. 7-4. Sixty-one rod cluster with 0·632 in. fuel spacing used in lattice 84 of the Savannah experiments (all dimensions are in inches).

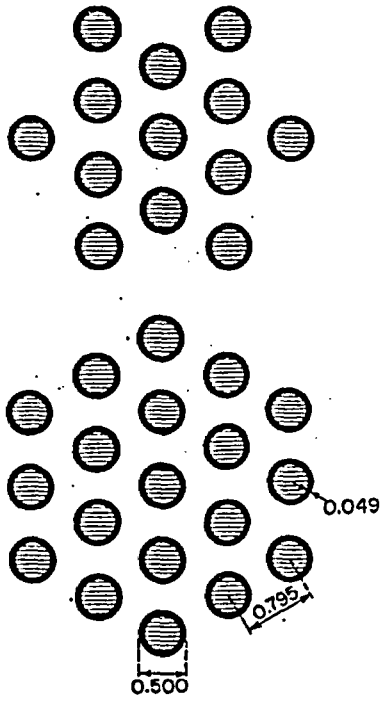

FIG. 7-5. Thirteen and nineteen rod clusters with 0·795 in. fuel spacings used in lattices 85 through 87 of the Savannah experiments (all dimensions are in inches).

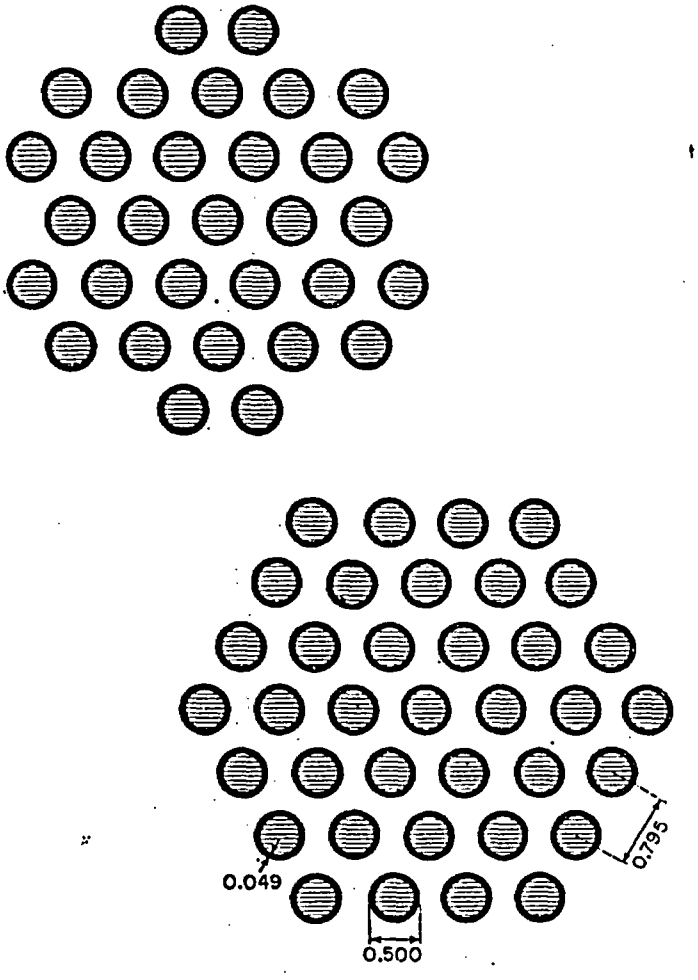

FIG. 7-6. Thirty-one and thirty-seven rod clusters with 0·795 in. fuel spacings used in lattices 88 through 93 of the Savannah experiments (all dimensions are in inches).

Bucklings

Because of the relatively small size of the test zone and the relatively small number of clusters present, a rather detailed and careful analysis was required. The Saclay lattice substitution experiment, although having data available for several sizes of the test zone, was guided somewhat by theory in obtaining buckling changes. However, the Savannah experiment must depend more heavily on reactor theory because of both the small size of the test zone and the fact that this size was held constant.

The basic approach of Dessauer's analysis[3] was to consider both resonance escape, p, and the buckling, B_1^2, of the central test lattice as unknowns, but related by either of the following critical equations,

$$\varepsilon_1 \eta_1 f_1 p_1 = (1+L_1^2B_1^2)(1+0{\cdot}378\tau_1 B_1^2)\exp(0{\cdot}622\tau_1 B_1^2) \quad (7\text{-}1)$$

$$\varepsilon_1\eta_1 f_1 p_1 = (1+L_1^2B_1^2)(1+\tau_1 B_1^2) \quad (7\text{-}2)$$

The former was used for metal fueled lattices, and the latter for oxide lattices presented here. Criticality of a two-group diffusion theory problem on the IBM 650 computer using the experimental geometry of the two-zone reactor was then a second condition to be satisfied. When B_1^2 and p_1 of the central zone satisfied both conditions, the buckling of the lattice had been determined.

If all the non-geometric parameters in the computer problem were obtained solely from reactor theory, the resulting B_1^2 would be strongly dependent on theory. However, fortunately p_2, L_2^2 and B_2^2 are known experimentally, for they are measured with the reference lattice occupying the entire PDP. Therefore, since B_1^2 depends strongly on B_2^2 and zone geometry and only to a lesser extent on other parameters, it can be said that B_1^2 is experimentally determined by this method, although theoretical corrections are far from negligible.

Typically the diffusion constants of the two regions are virtually equal in both groups, $D_{f1} = D_{f2}$ and $D_{s1} = D_{s2}$, and therefore do not influence the calculation. Although in the helium cooled lattices the non-equality of these was taken into account, this, nevertheless, represented a source of inaccuracy in the results for these lattices. Also, because of the small size of the central zone, care was taken to distinguish between the infinite lattice's resonance escape probability, p_1, and the finite lattice's value for this parameter to be used in the computation. These corrections have been

made on all the results reported here, though absent in some preliminary publications.[2]

Figures 7-7 to 7-10 display the results of these experiments, which are also given in Table 7-2. It is found more convenient here to show buckling variations at a constant cluster pitch, rather than for a constant number of fuel rods as in previous chapters. Buckling maxima are still exhibited. The gain in buckling of the 0·632 in. rod spacing over that of the 0·795 in. spacing against moderator to fuel

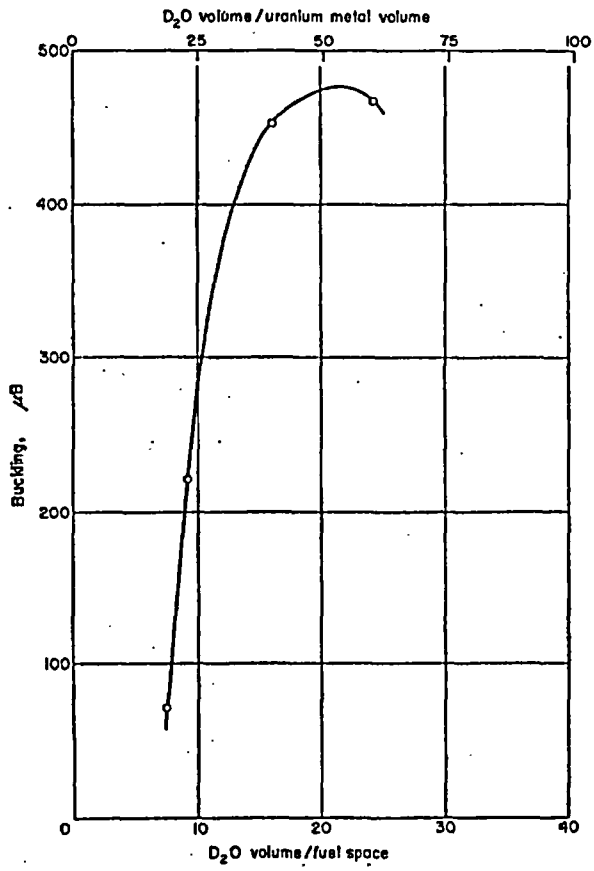

FIG. 7-7. Bucklings of 0·632 in. spaced rods in clusters spaced 7 in. (shown in Figs. 7-1 and 7-2).

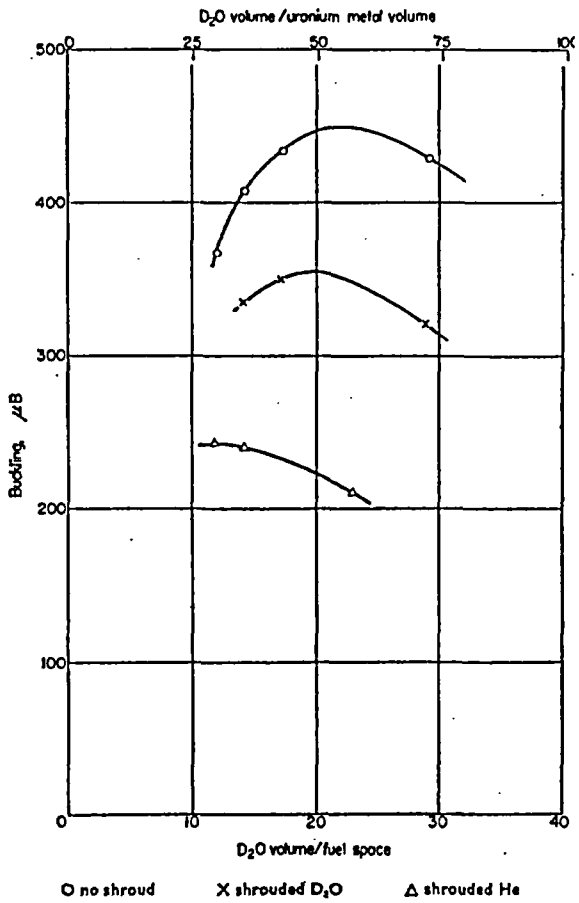

FIG. 7-8. Bucklings of 0·632 in. spaced rods in clusters spaced 9·26 in. (shown in Figs. 7-1 to 7-3).

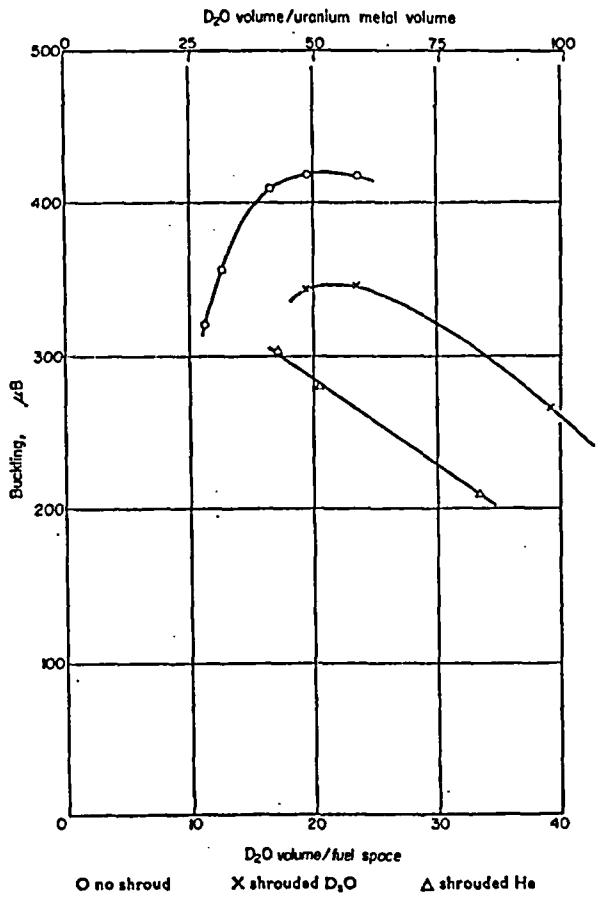

FIG. 7-9. Bucklings of 0·632 in. spaced rods in clusters spaced 10·7 in. (shown in Figs. 7-2 to 7-4).

influenced by voids in the coolant than outside the shroud. Negative void coefficient effects are dominating for these lattices.

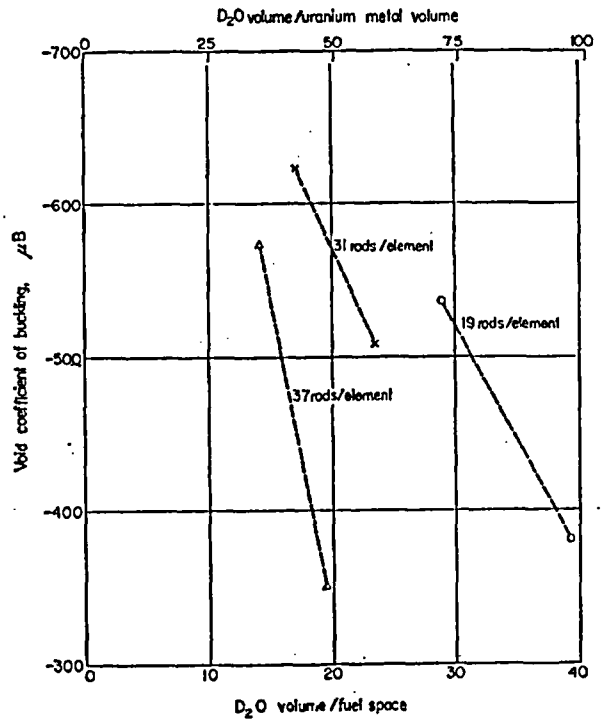

FIG. 7-12. Void coefficient of buckling for 0·632 in. spaced rods.

It is believed that the standard deviation of the buckling results is $\pm 25\mu B$. This was obtained by a statistical combining of random and systematic errors of all sources, particularly the following:

(a) lack of perfect reproducibility of moderator heights;
(b) assuming constant vertical reflector savings;
(c) using theoretical constants in arriving at bucklings;
(d) error in measuring the buckling of the outer region;
(e) errors in the corrections made.

Lattices 100 to 105 inclusive probably have a larger uncertainty than this $\pm 25\mu B$ because of their high void contents.

A systematic error in the use of the PDP to measure bucklings has been found, however, by Baumann.[4] In its ideal form the lattice substitution method of measuring bucklings uses a lattice in the outer zone which closely resembles the lattice being measured in the central zone. However, in the PDP the outer zone contained a heterogeneous mixture of poison rods and fuel rods. The relative thermal absorption between these poison rods in the outer zone and the fuel near the boundary of the central zone is influenced by the value of L^2 in the test lattice. This effect has not been corrected for in any of the data presented, but the corrections to be applied appear in Table 7-3.

TABLE 7-3. CORRECTIONS TO THE PDP BUCKLING MEASUREMENTS STEMMING FROM THE POISON ROD EFFECT

L^2 of test lattice in cm^2	The corrections, ΔB^2, in μB to be added to the measured buckling
45	10
80	0
180	−15
400	−30

The experiment was conducted with heavy water purities of 99·3 to 99·1 per cent, but all results reported have been corrected to 99·75 per cent. The temperature in all cases was 22°C.

Discussion

The purpose of the Savannah experiments was to make an extensive experimental buckling survey of a large number of lattices of practical interest to natural uranium fueled heavy water moderated power reactors. In order to survey more than 250 lattices in a relatively short time the most rapid technique compatible with adequate precision was used. This method is the lattice substitution experiment. Substitution of lattices into a central zone only 21 in. in diameter, though rapid, required as a consequence careful theoretical analysis and many corrections. Since the numerous results are believed reliable to $\pm$ 25μB, it appears that the experiment has achieved its goal.

Unfortunately, no direct comparison of bucklings of the lattices here with results for the same lattices by other techniques is possible. However, during the course of the experiment some uranium metal fueled lattices were measured, and compared favorably with their bucklings as determined by the SE.

REFERENCES

1. D. F. Babcock, Power reactor studies quarterly progress report, May, June and July (1957), DP-245. E. I. duPont, Wilmington, Delaware, September (1957).
2. D. F. Babcock, Power reactor studies quarterly progress report, August, September, and October (1957), DP-265. E. I. duPont, Wilmington, Delaware, February (1958).
3. G. Dessauer, Physics of natural uranium, D_2O lattices, P/590. Geneva conference (1958).
4. N. P. Baumann, Process development pile measurements of lattice parameters of natural uranium in heavy water, DP-407. E. I. duPont, Wilmington, Delaware, July (1959).

CHAPTER VIII

INTERPRETATION OF SAVANNAH $UO_2 - D_2O$ LATTICE EXPERIMENTS

Introduction

As pointed out in Chapter VII, the purpose of the Savannah experiments was to make an extensive survey of natural uranium – heavy water lattices. It follows, therefore, that the theoretical interpretation would, like the experiments, tend to be extensive in nature. This means simple, yet reasonably accurate, approximations would be used. It became possible to calculate many lattices with adequate precision without too much effort.

An important factor in the selection of the theoretical methods used was an immediate practical application of the study. The du Pont Company, at the request of the United States Atomic Energy Commission, was investigating power reactors moderated by heavy water and fueled with natural uranium.[1] The economics of particular reactor type is quite sensitive to criticality and fuel life physics calculations. Therefore, a theory was used which not only would correlate all the buckling measurements, but also would allow accurate extrapolation to conditions encountered in the power reactor being studied.

Buckling measurements unfortunately were made at room temperature in lattices free of fission products and plutonium. However, the buckling most needed in power reaction design is that at operating conditions at the end of the core's life. This is more important than knowing the "clean" (i.e. free of fission products and plutonium) lattice's buckling at room temperature or even at the operating temperature. In fact, the latter bucklings are rarely attained in practice due to the presence of control materials in the lattice initially. Thus it becomes the task of reactor physics not only accurately to correlate room temperature clean bucklings, but also to extrapolate these to bucklings of interest. Techniques used for the latter are beyond the scope of this chapter, but are as important as the former insofar as the ultimate practical application of the experiments is concerned.

The basic technique of analysis of the bucklings used by Dessauer *et al.*[2] is another variation on those already presented. Lattice constants calculated for the four factor formula were used with the experimental bucklings to determine an empirically adjusted parameter—in this case the resonance integral. With an eye towards future usefulness, simple, yet reasonably reliable, methods of arriving at the individual lattice constants were chosen. Upon obtaining the resonance integral for each fuel element, these could then be correlated with the effective surface to mass ratios of the fuel elements. The desired correlation of the experimental bucklings was thereby had in terms of an empirical formula for the resonance integral. Therefore this, used with the calculational methods, here gives a " best fit " to the measured bucklings.

One type of diffusion theory, leading to Equation (7-1), is a mixture of the two types already presented as leading to the critical equations, Equations (2-5) and (4-6). In the former a single group of fast neutrons diffused at constant energy. In the latter the Fermi ageing process was assumed to hold form fission energies down to thermal energies. In the following equations both processes are allowed in sequence:

$$D_s\nabla^2\phi_s-\sum_{as}\phi_s+q_r(\tau_r)=0 \tag{8-1}$$

$$\nabla^2 q_r=\frac{\partial q_r}{\partial\tau} \tag{8-2}$$

$$q_r(0)=p\sum_{sf}\phi_f \tag{8-3}$$

$$D_f\nabla^2\phi_f-\sum_{sf}\phi_f+\frac{k_\infty}{p}\sum_{as}\phi_s=0 \tag{8-4}$$

If $\nabla^2\phi$ and $\nabla^2 q$ are replaced by $-B^2\phi$ and $-B^2 q$ respectively, these equations are readily solved for the fluxes ϕ_s and ϕ_f, and the slowing down density, q_r:

$$\phi_s=\frac{q_r(\tau_r)}{\sum_{as}(1+L^2B^2)} \tag{8-5}$$

$$q_r(\tau_r)=q_r(0)\,e^{-\tau_r B^2} \tag{8-6}$$

$$q_r(0)=p\sum_{sf}\phi_f \tag{8-7}$$

$$\phi_f=\frac{k_\infty\sum_{as}\phi_s}{p\sum_{sf}(1+\tau_f B^2)} \tag{8-8}$$

The critical equation had by the elimination of the fluxes and slowing down density is

$$k_\infty = (1+L^2B^2)\,e^{\tau_r B^2}\,(1+\tau_f B^2) \tag{8-9}$$

There is some evidence[3] that the ageing process may be better described in the dual form of Equation (8-9) than that used in previous chapters,

$$k_\infty = (1+L^2B^2)(1+\tau B^2) \tag{8-10}$$

or

$$k_\infty = (1+L^2B^2)\,e^{\tau B^2} \tag{8-11}$$

It is evident that with

$$\tau = \tau_r + \tau_f \tag{8-12}$$

Equation (8-9) is bracketed by the other forms, Equations (8-10) and (8-11).

To estimate the effect of using different critical equations, consider the latter pair for a typical natural uranium lattice in which

$$L^2 = 150\ \text{cm}^2 \tag{8-13}$$

$$\tau = 130\ \text{cm}^2 \tag{8-14}$$

$$B^2 = 200\ \mu\text{B to } 600\ \mu\text{B} \tag{8-15}$$

The quotient of the right-hand sides of Equations (8-10) and (8-11) is

$$\frac{1{\cdot}03\times 1{\cdot}02600}{1{\cdot}03\times 1{\cdot}02634} = 0{\cdot}99967 \tag{8-16}$$

and

$$\frac{1{\cdot}09\times 1{\cdot}07800}{1{\cdot}09\times 1{\cdot}08112} = 0{\cdot}99711 \tag{8-17}$$

for these two bucklings. Thus, reactivity differences as low as 0·033 per cent or as large as 0·29 per cent can be had. The differences in calculating buckling from Equations (8-10) or (8-11) are

$$\frac{0{\cdot}033\times 10^{-2}}{280} = 1{\cdot}2\ \mu\text{B} \tag{8-18}$$

and

$$\frac{0{\cdot}29\times 10^{-2}}{280} = 10\ \mu\text{B} \tag{8-19}$$

if $M^2 \cong 280\,\text{cm}^2$ is typical.

Thus, the various interpretations of the ageing process differ typically by less than the precision to which the lattice constants are known. It is only for lattice types having a large value of τB^2 that these differences become important. As mentioned in Chapter VII, the oxide lattices treated here were analyzed by Equation (8-10), while other metal fueled lattices were analyzed by Equation (8-9).

Fast effect

The formula used for calculating the fast fission factor, ε, is

$$\varepsilon = 1 + \frac{\nu_f - 1}{\nu} \mathscr{R} \tag{8-20}$$

where $\mathscr{R}$ is the fast to thermal fission ratio. $\mathscr{R}$ was computed by essentially Spinrad's method,[4] after homogenizing the fuel element. For uranium metal rods, measurements of $\mathscr{R}$ were useful in verifying the calculational technique.

Comparison of Equation (8-20) with either Equations (4-7) or (6-2) indicates that simplifying assumptions have been made. In particular, the non-fission capture that was not taken into account in calculating ε was subsequently included in the calculation of p. This was convenient, because the resonance integral was empirically determined in this analysis.

Values of ε in Table 8-1 are plotted in Fig. 8-1. The fast effect

TABLE 8-1. CALCULATED LATTICE CONSTANTS AND EXPERIMENTAL BUCKLINGS OF THE SAVANNAH LATTICES

Lattice No.	ε	f	p	L^2 in cm²	τ in cm²	B^2 in μB
72	1·011	0·929	0·931	196	135	466
73	1·013	0·934	0·901	139	142	452
74	1·013	0·923	0·945	255	133	429
75	1·014	0·939	0·835	87	156	221
76	1·014	0·932	0·907	166	140	433
77	1·014	0·925	0·930	231	136	417
78	1·015	0·940	0·803	74	163	71
79	1·015	0·934	0·890	141	144	408
80	1·015	0·929	0·916	198	138	418
81	1·015	0·936	0·875	123	148	367
82	1·015	0·931	0·903	173	141	409
83	1·016	0·934	0·877	139	147	356
84	1·016	0·935	0·865	126	150	320
85	1·007	0·929	0·924	184	135	444
86	1·007	0·934	0·892	128	142	409
87	1·007	0·924	0·938	236	133	413
88	1·008	0·939	0·818	78	156	116
89	1·008	0·932	0·898	149	140	402
90	1·008	0·926	0·922	208	136	403
91	1·008	0·940	0·779	65	163	−94
92	1·008	0·934	0·879	125	144	356
93	1·008	0·929	0·907	176	138	395

increases with the number of rods in the cluster and is larger for the tighter spacing.

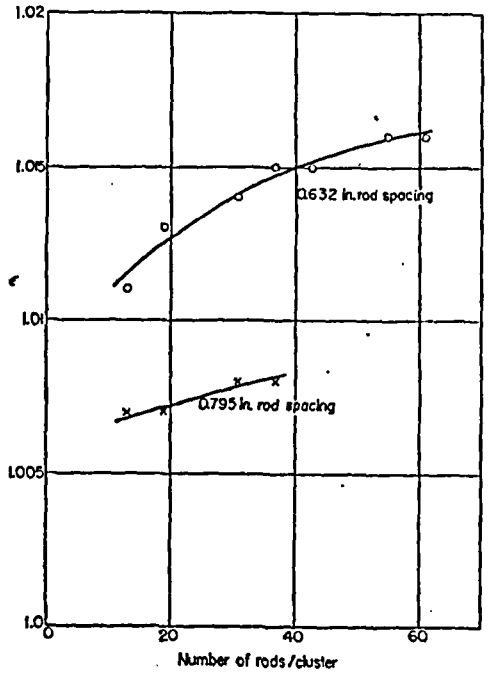

FIG. 8-1. The fast effect for lattices 72 to 93.

Resonance escape

The method used for calculating p was the single energy method of Critoph,[5] already introduced in Chapter VI. In this method all the resonance capture is assumed to occur at a single energy, E_R. By this simplification it is possible to treat heterogeneous effects quite accurately. However, since E_R is an unknown, it was necessary to perform the resonance escape calculations for more than one assumption for E_R.

σ_{ar}, the resonance integral, was taken to be the parameter to be determined in order to fit the theory to the experiment. It was had by first obtaining $1-p$ from the experimental buckling and the calculated values for the other lattice constants. Then for a given E_R by using Critoph's method, σ_{ar} could be determined.

In order to correlate the σ_{ar}'s of the various fuel elements som dependence on the fuel element parameters must then be assumed:

$$\sigma_{ar} = \frac{\mathscr{A}}{[\kappa_r r_f I_0(\kappa_r r_f)]/[2I_1(\kappa_r r_f)]} + \mathscr{B}\frac{S_{eff}}{M} \tag{8-21}$$

Here $\kappa_r r_f I_0(\kappa_r r_f)/2I_1(\kappa_r r_f)$ is the surface to average interior resonance flux ratio, and $\mathscr{A}$ and $\mathscr{B}$ are constants to be determined from a plot of σ_{ar}'s evaluated against S_{eff}/M. The effective surface of the fuel in a cluster was taken to be the outer surface plus the corrected inner surface. The latter is the Dancoff corrected inner surface times the interior to surface flux ratio.

Thermal utilization and η

In the formula for thermal utilization,

$$f = \frac{(\sum_{as\,235} V_{235} + \sum_{as\,238} V_{238})\phi_{s\,\mathrm{fuel}}}{\sum_i \sum_{as\,i} V_i \phi_{s\,i}} \tag{8-22}$$

Dessauer *et al.* chose the P_3 spherical harmonics method[6] as the means for computing the flux ratios, $\phi_{s\,i}/\phi_{s\,\mathrm{fuel}}$. For those lattices in which this quantity was measured, agreement was found with the results of the P_3 method, within the experimental error. Table 8-1 contains the values of f computed.

Motivated by the desire for simple methods that would be of practical use for extensively surveying many lattices, the Savannah group chose η to be its value in a well thermalized spectrum for natural uranium, namely 1·327.[7] However, according to Equation (4-14), η in fact depends on the ratio of U^{235} to U^{238} absorption cross-sections. Since the former falls off with energy faster than $1/v$, lattices having " harder " spectra tend to have lower effective values of η. The more tightly spaced lattices have harder spectra, i.e. a higher mean neutron temperature, because the higher thermal absorption tends to remove the lower energy neutrons from the approximately Maxwellian spectrum.

It was within the spirit of the approximations made to use a constant η, and allow its variation with spectra to be reflected as a variation in σ_{ar}. This is because not only is the spectral dependence of η approximated as a constant here, but the relative effectiveness of epithermal and thermal fissions is also taken to be the same. The latter is a consequence of the assumption of a single fissioning group in Equations (8-1) to (8-4).

Migration area

An approximate formula for age can be had by setting $\mathscr{P} = 0$ in Equation (6-18), and instead taking into account the uranium moderation by an approximate assumption about cross-sections:

$$\tau = \frac{\sum_i V_i}{D_{fM} \sum_i V_i D_{fi}^{-1}} \frac{\sum_i V_i}{(\xi \sum_s)_M^{-1} \sum_i V_i (\xi \sum_s)_i} \tau_M \tag{8-23}$$

$$\tau \cong \tau_M \left(1 + \frac{V_U}{\sum_i V_i}\right)\left(1 + 2\frac{V_{Al} + V_V}{\sum_i V_i}\right) \tag{8-24}$$

Here V_U is the volume of equivalent uranium metal obtained from V_F by requiring the equivalent metal to occupy a volume having the same number of uranium atoms; V_V is the sum of the actual void volume and $V_F - V_U$.

In these equations the transport and slowing down cross-sections of the uranium are taken to be half those of the heavy water, while those of the aluminum are ignored. In addition, terms of order $(V_U/\sum V_i)^2$ are ignored. $120\,\text{cm}^2$ is the value used for the heavy water age, τ_M. The division of the total age, τ, into τ_r and τ_f was accomplished by[3]:

$$\tau_r = 0{\cdot}622\tau \tag{8-25}$$

$$\tau_f = 0{\cdot}378\tau \tag{8-26}$$

L^2 was computed from the flux and volume weighed transport and absorption cross-sections:

$$L^2 = \frac{1}{3\overline{\sum}_{trs}\overline{\sum}_{as}} \tag{8-27}$$

According to Table 8-1 there is an appreciable variation in L^2 among the lattices. τ does not appreciably exceed the age of pure heavy water because the uranium and aluminum occupy such a small fraction of the lattice. However, L^2 by virtue of its inverse dependence on $\overline{\sum}_{as}$ is approximately proportional to $\phi_M V_M/\phi_F V_F$. This is shown in Fig. 8-2. The larger fuel element spacings have a larger ratio of ϕ_M/ϕ_F for a given V_M/V_F, and hence a larger L^2.

Since the Savannah lattices 100 to 105 contained helium, a correction of both τ and L^2 must be made for the effect known as steaming. Basically the above formulae are applicable to a homogeneous

mixture of materials, although in L^2 the thermal flux heterogenuities are taken into account. However, in practice the discrete lumping of the fuel in all lattices and of the helium in a few lattices leads to two effects,

(a) Anisotropic leakage: The leakage in the direction parallel to the fuel or void axis tends to be enhanced, as illustrated in Fig. 8-3.

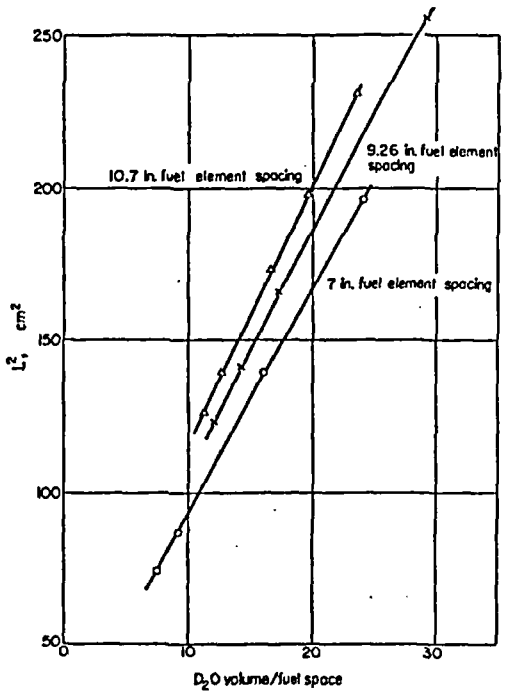

FIG. 8-2. The dependence of L^2 on the moderator to fuel ratio for lattices 72 to 84.

(b) Enhanced leakage: If two lattices have the same volume ratios among materials, the one having the larger degree of lumping has the larger leakage. This is due to the larger migration area as illustrated in Fig. 8-4.

Correcting τ and L^2 for the heterogenuities of the fuel and aluminum is complex, and probably negligible for most lattices.

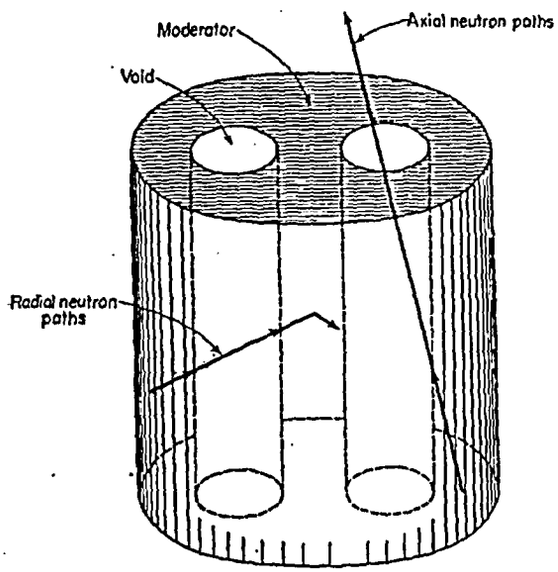

FIG. 8-3. Neutron streaming causing greater axial leakage than radial. Those neutrons which are oriented mostly in the z direction tend to travel further than those radially oriented because of the probability of long unimpeded paths almost vertically in the voided region.

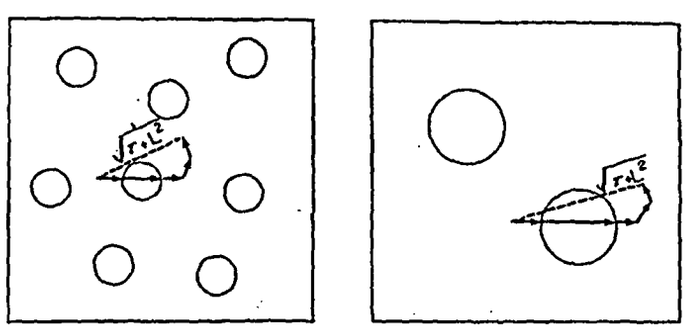

FIG. 8-4. Larger migration area due to void heterogenuities. Although the two lattices have the same void fraction, the lower has the larger migration area because of the increased probability of the neutrons having long unimpeded paths through the void.

However, the lattices with the gas coolant are readily corrected by the formula of Behrens[8]:

$$\frac{\text{corrected } L_z^2}{\text{homogeneous } L_z^2} = \frac{1+2F+F\sum_{trs} a\left[\left(\text{cotanh}\,\frac{\sum_{trs} a}{F}\right)+1\right]}{1+2F+F^2} \tag{8-28}$$

$$\frac{\text{corrected } L_r^2}{\text{homogeneous } L_r^2} = \frac{1+2F+F\sum_{trs} a\,\text{cotanh}\,\frac{\sum_{trs} a}{F}}{1+2F+F^2} \tag{8-29}$$

where F is the void to non-void ratio in the lattice having voided cylinders of radius, a. The age is corrected by a similar formula. This anisotropic migration is used to compute leakage as already shown in Equation (3-9).

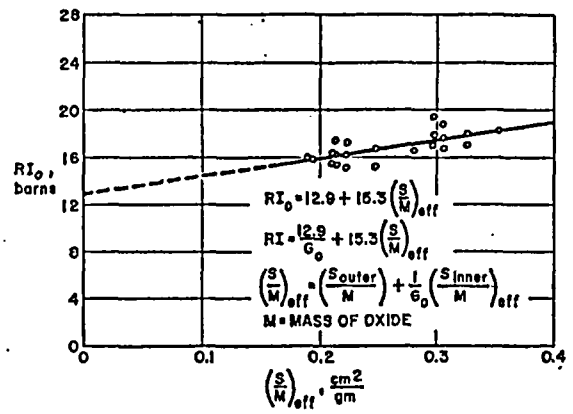

FIG. 8-5. σ_{ar}, the effective resonance integral of uranium oxide, (RI).

Analysis of bucklings

The steps used in the analysis of the measured bucklings consisted in: obtaining p and the buckling as previously described; then obtaining σ_{ar} from the formula for p, using various values for E_R. Figure 8-5 shows a plot of the σ_{ar}'s obtained for $E_R = 30\,\text{eV}$ and the determination of $\mathscr{A}$ and $\mathscr{B}$ in Equation (8-21). It was found that $E_R = 30\,\text{eV}$ gave the least scatter of points in this type of plot.

The resonance integral obtained differs significantly in S_{eff}/M dependence had from direct measurements[9] used by Critoph in Chapter VI, which give

$$\sigma_{ar} = \frac{10{\cdot}1}{[\kappa_r r_{f0} I_0(\kappa_r r_{f0})]/[2I_1(\kappa_r r_{f0})]} + 30{\cdot}0\,\frac{S_{eff}}{M}\ \text{barns} \tag{8-30}$$

However, for $S_{eff}/M = 0{\cdot}25$, Fig. 8-5 gives 16·7, while Equation (8-30) gives 17·6 barns. This is some indication of the overall consistency of the Savannah methods of calculation.

Another indication of the combined consistency of the buckling measurements and theoretical methods is the average deviation of the points in Fig. 8-5, which is about $\pm$ 0·6 barn in 17 barns. This corresponds to about a $\pm$ 0·6 per cent dispersion in $k\infty$, a typical value of which is 1·1. This in turn, corresponds to about a $\pm$ 6 per cent dispersion in bucklings in the vicinity of 400μB. It has already been noted in Chapter VII that buckling measurements are accurate to $\pm$ 25μB. Thus, Fig. 8-5 is a further confirmation of this degree of precision. It is interesting to note that correlations as Fig. 8-5 (or η calculations as in Chapter IV) show very nicely the statistical uncertainties in buckling measurements, provided fluctuations due to the theory are small. Whereas the conventional presentations of buckling versus moderator to fuel ratio do not show this.

Dessauer has actually tested the dispersion of the experimental bucklings in a more precise way. When the bucklings calculated by the use of the resonance integral formula found in Fig. 8-5 were compared with those measured, a standard deviation of 21μB was had.

REFERENCES

1. D. F. Babcock, Heavy water moderated power reactors, P/610. Geneva conference (1958).
2. G. Dessauer, Physics of natural uranium D_2O lattices, P/590. Geneva conference (1958).
3. F. L. Friedman and A. Wattenberg, The slowing down of neutrons in heavy water, CP-3453 (1946).
4. B. I. Spinrad, Fast effect in lattice reactors, NSE 1, 455 (1956).
5. E. Critoph, Comparison of theory and experiment for: (a) Lattice properties of D_2O–U reactors; (b) Central rod experiments; (c) Foreign rod experiments, CRRP-655, AECL No. 350 (1956).
6. B. Davison, *Neutron Transport Theory*, p. 116. Oxford (1957).
7. D. J. Hughes and J. A. Harvey, Neutron cross-sections, BNL-325 (1955).
8. D. J. Behrens, The Migration length of neutrons in a reactor, AERE T/R 877 (1952).
9. E. Hellstrand, Measurements of the effective resonance integral in uranium metal and oxide in different geometries. *J. Appl. Phys.* 28, 1493 (1957).